Isolation of PPFIBP1–ALK fusion

To obtain cDNA fragments corresponding to a novel *ALK* fusion gene, we used a 5′-RACE method with the SMART RACE cDNA Amplification Kit (Clontech) according to the manufacturer's instructions, with a minor modification: the ALK2458R primer (5′-GTAGTTGGGGTTGTAGTCGGTCATGATGGT-3′) was used as the gene-specific reverse primer.

From the oligo(dT)-primed cDNA obtained from case 2 RNA, a 471bp cDNA fragment containing the fusion point was specifically amplified with the primers PPFIBP1-592F (5′-AGAGACACAGAGGGGCTGATT-3′) and ALK3078RR (5′-ATCCAGTTCGTCCTGTTCAGAGC-3′).

PCR analysis of genomic DNA for *PPFIBP1–ALK* in case 2 was carried out with a pair of primers flanking the putative fusion point, PPFIBP1-607F (5′-CTGATTCAGGAGATCAATGATTTGAGGT-3′) and Fusion-RT-AS (5′-TCTTGCCAGCAAAGCAGTAGTTGG-3′).

From the cDNA, a full-length cDNA for *PPFIBP1–ALK* was amplified by PCR with the PA-w-cDNA-in-S primer (5′-TATCTGGGTTGGAATTTGCCCCTG-3′) and the KA-w-cDNA-in-AS primer (5′-TGAGTGTGCGACCGAGCTCAGG-3′) and PrimeSTAR HS DNA polymerase (TakaraBio).

FISH

FISH analysis of gene fusion was carried out with bacterial artificial chromosome (BAC) clone-derived DNA probes for *ALK* and *PPFIBP1*. Unstained sections (4 μm thick) were subjected to hybridization with an *ALK*-split probe set (Abbott) or BAC clone-derived probes for *ALK* (RP11-984I21, RP11-62B19) and *PPFIBP1* (RP11-1060J15). Hybridized slides were then stained with DAPI and examined with the fluorescence microscope BX51 (Olympus).

Transformation assay for ALK fusion proteins

Analysis of the transforming activity of PPFIBP1–ALK was carried out as described previously (20, 37, 38). Briefly, the pMXS-based expression plasmid for PPFIBP1–ALK, EML4–ALK variant 1, or NPM–ALK was used to generate recombinant ecotropic retrovirus, followed by individual infection of mouse 3T3 fibroblasts (39). Formation of the transformed foci was evaluated after culturing the cells for 14 days. The same set of 3T3 cells was subcutaneously injected into nu/nu mice, and tumor formation was examined after 20 days. The animal experiments were approved by the animal ethics committee of Jichi Medical University.

Results

Morphology and immunophenotype of PPFIBP1–ALK-positive IMT

Histopathologic analysis of the 2 IMT cases revealed a marked proliferation of cells composed of somewhat histiocytoid spindle cells showing a fascicular or storiform pattern. The tumor cells were uniform and had pale eosinophilic cytoplasm and an oval vesicular nucleus, within which a small nucleolus was centrally located. Mild inflammatory infiltrate containing lymphocytes, plasma cells, foamy histiocytes, and multinucleated giant cells was observed (Fig. 1A and 1D). The immunophenotype of the 2 cases was negative for smooth muscle actin,

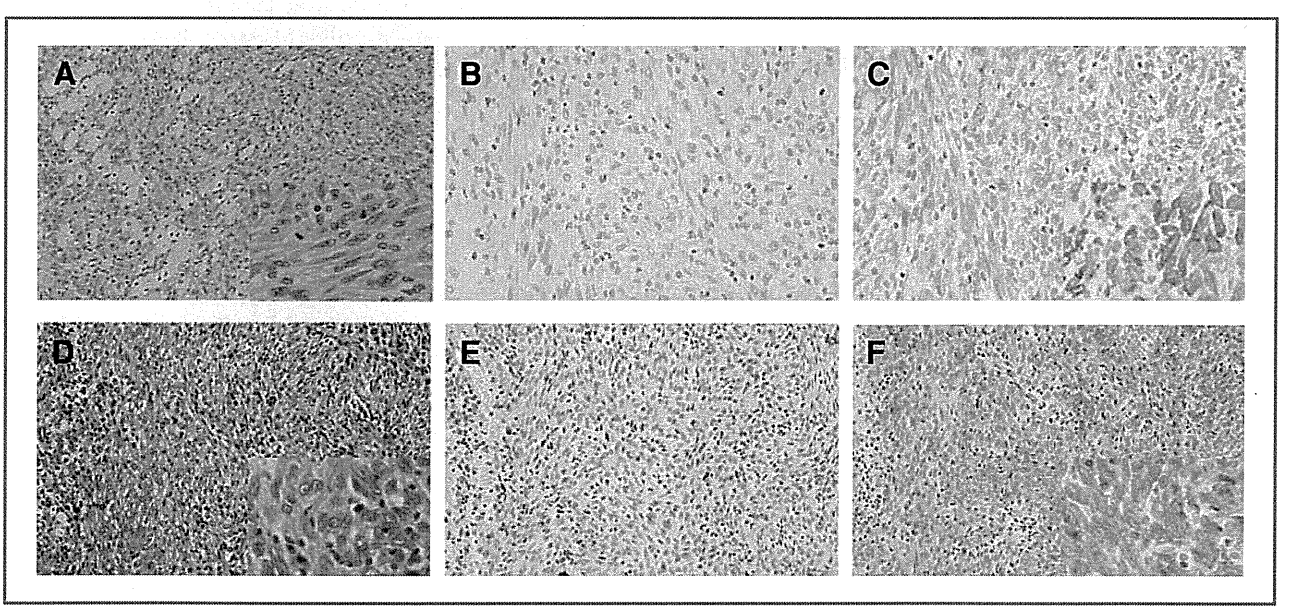

Figure 1. Histopathology of PPFIBP1–ALK-positive IMT. Diffuse proliferation of histiocytoid spindle cells showing a fascicular or storiform pattern. The tumor cells were uniform and had pale eosinophilic cytoplasm and an oval vesicular nucleus, within which a small nucleolus was centrally located. Mild inflammatory infiltrate containing lymphocytes, plasma cells, and foamy histiocytes is observed (A and D). The tumor cells were negative for ALK with conventional anti-ALK immunohistochemistry (B and E), but were clearly positive for ALK when the iAEP method was used. The staining pattern is diffuse cytoplasmic (C and F). Case 1 (A–C), Case 2 (D–F).

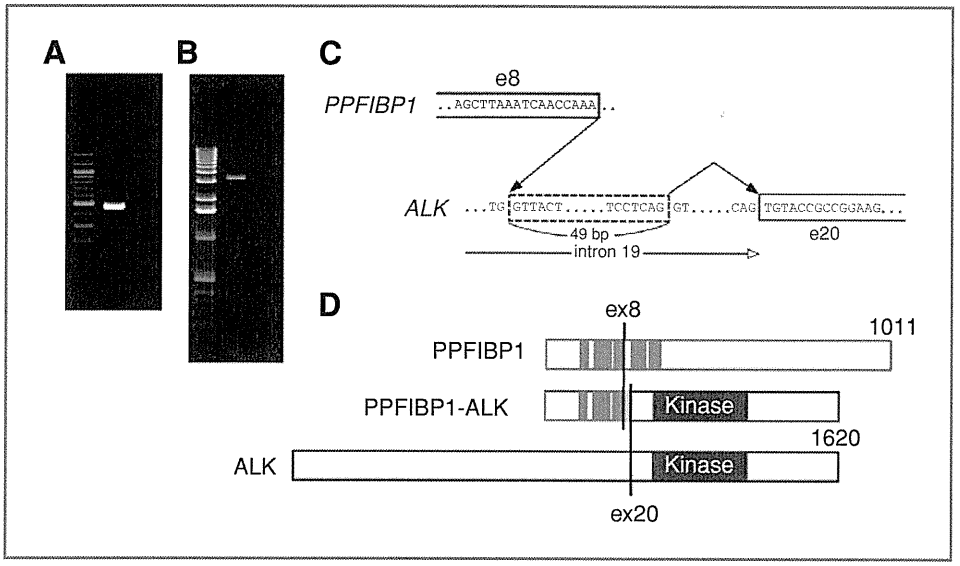

Figure 2. Identification of PPFIBP1–ALK: a PCR product of 471 bp covering the fusion point of *PPFIBP1–ALK* cDNA was specifically amplified from the tumor cells of case 2. The left lane contains DNA size standards (100 bp ladder). The right lane represents no template control (A). A PCR product of approximately 3 kbp covering the genomic fusion point of *PPFIBP1–ALK* was specifically amplified from the tumor cells of case 2. The left lane contains DNA size standards (1 kbp ladder). The right lane represents no template control (B). In our 5′-RACE products, exon 8 of *PPFIBP1* cDNA was fused to a 49 bp sequence in intron 19 of *ALK*, followed by exon 20 of *ALK* (C). PPFIBP1 contains 5 coiled-coil domains. A chromosome translocation, t(2;10)(p23;p11), generates a fusion protein in which the top 3 coiled-coil domains of PPFIBP1 and the intracellular region of ALK (containing the tyrosine kinase domain) are conserved. Numbers indicate amino acid positions of each protein (D).

HHF35, CD34, AE1/AE3, and S100. Desmin was focally positive in case 1, but was negative in case 2.

Identification of PPFIBP1–ALK as a novel ALK fusion gene

We conducted anti-ALK immunohistochemistry on 2 morphologically typical pulmonary IMT cases, originally diagnosed as fibrous histiocytoma. Immunostaining for ALK with the conventional polymer method led to the revised diagnosis of "ALK-negative" IMT (Fig. 1B and E). In the present study, anti-ALK immunohistochemistry with the iAEP method, however, showed a diffuse positive cytoplasmic staining (Fig. 1C and F), indicating the possibility of ALK fusion to a novel partner gene, the expression level of which is modest. To address this issue, in case 2 we conducted 5′-RACE assay for the isolation of an upstream cDNA to the ALK kinase domain cDNA, for which snap-frozen material was available.

Interestingly, we isolated a cDNA fragment containing exon 8 of *PPFIBP1* followed by a 49 bp-sequence within intron 19 of *ALK* and coupled to exon 20 of *ALK* (Fig. 2), suggesting the presence of a novel fusion between *PPFIBP1* and *ALK* genes. Because insertion of the intronic 49 bp allows an in-frame fusion between the 2 genes, this rearrangement likely produces a novel fusion-type tyrosine kinase. To confirm the genomic rearrangement responsible for the *PPFIBP1–ALK* fusion, a genomic PCR assay (Fig. 2B) and both *ALK* split and *PPFIBP1–ALK* fusion FISH assays (Fig. 3) were carried out. All results were consistent with the presence of t(2;12)(p23;p11) leading to the generation of *PPFIBP1–ALK*. Owing to the limited material available in case 1, only the FISH analyses were carried out. Surprisingly, these results also indicate the presence of *PPFIBP1–ALK* (Fig. 3, Supplementary Fig. 2A–C).

Transforming activities of PPFIBP1–ALK

To prove that the t(2;12)(p23;p11) rearrangement leads to the production of PPFIBP1–ALK kinase, in case 2 we attempted to amplify from the cDNA a full-length cDNA encoding the protein. By using a sense primer at the 5′-untranslated region of *PPFIBP1* mRNA (GenBank accession no. NM_003622) and an antisense primer at

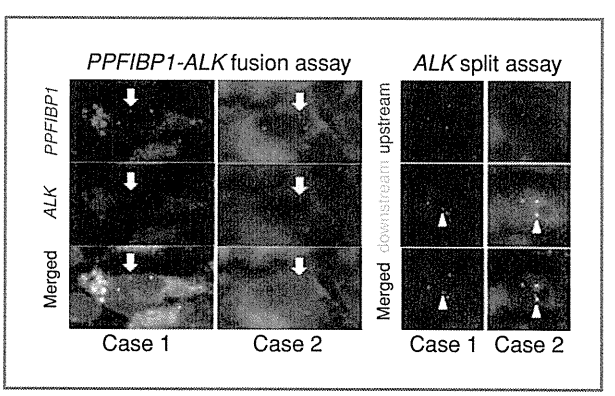

Figure 3. FISH analyses for *PPFIBP1–ALK*: sections of tumors positive for PPFIBP1–ALK were subjected to FISH analyses. In *PPFIBP1–ALK* fusion assays (left) the fusion genes are indicated by arrows. In *ALK* split assays (right) the 3′-sides of *ALK* are indicated by arrowheads. The color of fluorescence for the BAC clones and the case numbers in each hybridization are indicated. Nuclei are stained blue with DAPI.

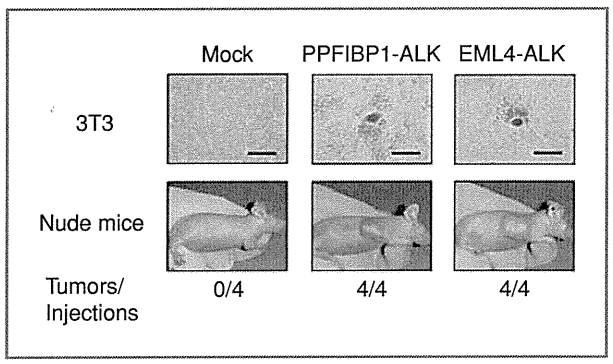

Figure 4. Transforming potential of PPFIBP1–ALK. Top, mouse 3T3 fibroblasts were infected with retroviruses encoding PPFIBP1–ALK or EML4–ALK or with the corresponding empty virus (Mock). The cells were photographed after 14 days of culture. Scale bars, 400 μm. Bottom, Nude mice were injected subcutaneously with the corresponding 3T3 cells, and tumor formation was examined after 14 days. The number of tumors formed per 4 injections is indicated at the bottom.

the 3′-untranslated region of *ALK* mRNA (GenBank accession no. NM_004304), a full-length *PPFIBP1–ALK* cDNA of 2488 bp was successfully amplified, which should have produced a fusion kinase of 811 amino acids with a predicted molecular weight of 90,740 Da (Supplementary Fig. 1).

To examine the transforming potential of PPFIBP1–ALK, a recombinant ecotropic retrovirus was generated to express PPFIBP1–ALK, which was used to infect mouse 3T3 fibroblasts. As shown in Figure 4, PPFIBP1–ALK produced hundreds of transformed foci over 14 days of culture, which was comparable with the observation with EML4–ALK. Furthermore, subcutaneous injection of the infected 3T3 cells into the shoulder of nude mice revealed that those expressing either PPFIBP1–ALK or EML4–ALK formed large tumors *in vivo*.

Discussion

Since their discovery in 1994, appropriate diagnosis of ALK fusion-positive tumors with conventional anti-ALK immunohistochemistry methods has been accepted. However, EML4–ALK in lung adenocarcinoma, identified in 2007, did not stain positive for ALK with conventional immunohistochemistry methods (21, 35). We developed a sensitive immunohistochemistry method, the iAEP method, and successfully stained EML4–ALK with ordinary anti-ALK mouse monoclonal antibodies (21, 31–33). Such observation further indicates a possibility that staining cancer specimens with sensitive immunohistochemical methods (such as iAEP) may detect novel ALK fusions in the "ALK-negative" tumors defined by conventional anti-ALK immunohistochemistry methods. On the basis of this hypothesis, we have identified a novel ALK fusion in "ALK-negative" IMT.

Caution is needed in practical settings. For example, rhabdomyosarcoma, especially of the alveolar type, often expresses wild-type ALK at a detectable level with conventional anti-ALK immunohistochemistry (40). Moreover, in our experience, a small portion of small cell carcinoma and large cell endocrine carcinoma of the lung, and some sarcomas, may be positive for ALK by iAEP immunohistochemistry, expressing wild-type ALK. Therefore, in order to specifically detect ALK fusions with sensitive anti-ALK immunohistochemistry, a confirmatory test by using FISH, RT-PCR, or similar is usually required. If a tumor is positive for a confirmatory test and the suspected partner gene is not a reported one, 5′-RACE or inverse reverse transcriptase PCR methods can be used for the identification of the suspected partner. Even if overexpressed, wild-type ALK may not be oncogenic (20, 21, 37, 38), although some investigators have suggested that wild-type ALK overexpression above a certain threshold level drives the growth of neuroblastoma (41). Further investigation will be required to clarify if wild-type ALK overexpression is a target for ALK inhibitor therapy.

IMT is a rare mesenchymal tumor that has been referred to as inflammatory pseudotumor, plasma cell granuloma, fibroxanthoma, fibrous histiocytoma, pseudosarcomatous myofibroblastic tumor, and invasive fibrous tumor of the tracheobronchial tree (42). It occurs in the soft tissues as well as in the viscera and the lung, and is more likely to occur in children and young adults. Histologically, IMT is composed of a variable admixture of bland, spindle-shaped myofibroblast-like cells and an inflammatory component of lymphocytes, eosinophils, plasma cells, and macrophages. Recent genetic studies have elucidated clonal chromosomal abnormality involving 2p23, at which ALK is located, in a subset of IMT. The expression of ALK fusion proteins is detected by anti-ALK immunohistochemistry in approximately 50% of IMT cases (42), in which various ALK fusion genes have been reported (Table 1). Collectively, these lines of evidence support ALK-positive IMT being a distinct neoplastic entity. However, the other 50% of IMT cases are negative for anti-ALK immunohistochemistry, and thus in terms of pathogenesis it remains unknown whether these ALK-negative IMTs should be included in the same entity or not. In fact, 1 ALK-negative IMT case did not respond to crizotinib therapy (29). However, we have detected a novel ALK-fusion in "ALK-negative" IMT that subsequently proved positive for ALK with the iAEP immunohistochemistry method. Therefore, unexpectedly lowly expressed ALK fusions may explain the pathogenesis of a portion of "ALK-negative" IMT cases. PPFIBP1–ALK represents such an ALK fusion, although we do not yet know what proportion of "ALK-negative" IMTs can be attributed to this novel subtype. "ALK-negative" IMT warrants screening with the iAEP method to detect this fusion or other, unrecognized, ALK fusions.

PPFIBP1 codes liprin beta 1 (also called PTPRF-interacting protein-binding protein 1). This 114 kDa protein is a member of the leukocyte common antigen–related (LAR) transmembrane tyrosine phosphatase-interacting protein family that may regulate LAR protein properties via interaction with another member of the family, liprin alpha1 (43). Liprin beta 1 expresses in intestinal lymphatic endothelial cells *in vitro* and lymphatic vasculature *in vivo*,

Table 1. ALK fusion partners in well-documented IMT cases

Partner	Locus	Age	Sex	Site	Year, First author
TPM3	1p23	30	F	Lung	2000, Lawrence
		23	F	Abdomen	2000, Lawrence
		4	M	Lung	2006, Yamamoto
		29	F	Ileum	2006, Milne
		4	M	Lung	2007, Kinoshita
TPM4	19p13	1	M	Abdomen	2000, Lawrence
		6	M	Mesentery	2003, Hisaoka
		25	M	Prostate	2003, Hisaoka
		5	M	Mesentery	2006, Yamamoto
		5	F	Urinary bladder	2006, Yamamoto
CLTC	17q23	3	F	Neck	2001, Bridge
		37	M	Pelvis	2001, Bridge
		2	M	Thoracic cavity	2006, Yamamoto
		6	M	Mesentery	2006, Yamamoto
		0	F	Mediastinum	2007, Patel
CARS	11p15	0	M	Abdomen	2002, Cools
		10	M	Neck	2003, Debelenko
RANBP2	2q13	7	M	Abdomen	2003, Ma
		0	M	Abdomen	2003, Ma
		2	M	Abdomen	2007, Patel
		34	M	Liver	2008, Chen
		44	M	Abdomen	2010, Butrynski
ATIC	2q35	46	M	Urinary bladder	2003, Debiec-Rychter
SEC31L1	4q21	23	M	Abdomen	2006, Panagopoulos
PPFIBP1	12p11	45	M	Lung	Present case 1
		34	F	Lung	Present case 2

and plays an important role in the maintenance of lymphatic vessel integrity in *Xenopus* tadpoles (44). PPFIBP1 has 5 coiled-coil domains in exons 5 through 12, and the upper 3 domains are conserved in fusion form with ALK (Fig. 2D). The coiled-coil domain is shared in all ALK fusion partners (except for NPM, MSN, and SQSTM1), with which the ALK fusion proteins homodimerize leading to constitutive activation of ALK kinase domains (8, 19). As expected, in the present study, the oncogenicity of PPFIBP1–ALK was clearly confirmed with an *in vitro* focus formation assay and an *in vivo* tumorigenicity assay.

The difference in subcellular localization has contributed to the discovery/identification of various ALK fusions. Likewise, the difference in the expression level found is here proved important in the accurate detection of fusion proteins. Sensitive immunohistochemical methods such as iAEP will broaden the potential value of immunohistochemistry, which is a simple and long-established histopathologic technique in the fields of research and diagnosis. The ALK positivity rate (approximately 50%) in IMT should be reassessed with these more sensitive methods, possibly leading to the identification of novel ALK fusions and more candidates for ALK inhibitor therapy. A novel ALK fusion, VCL–ALK, has recently been identified in renal cancers (45, 46). In addition to IMT, therefore, a reassessment of diverse "ALK-negative" human cancers may be required in the forthcoming era of ALK inhibitor therapy.

Disclosure of Potential Conflicts of Interest

K. Takeuchi, scientific advisor for developing an anti-ALK iAEP immunohistochemistry kit (ALK Detection Kit, Nichirei Bioscience, Japan) and in charge of pathology screening for ALK fusions using the immunohistochemistry kit and an original probe set for ALK split FISH assay in a clinical trial of an ALK inhibitor (AF802, Chugai, Japan). The other authors disclosed no potential conflicts of interest.

Grant Support

This work was supported in part by Grants-in-Aid for Scientific Research from the Ministry of Education, Culture, Sports, Science, and Technology of Japan as well as by grants from the Japan Society for the Promotion of Science; the Ministry of Health, Labor, and Welfare of Japan; the Vehicle Racing Commemorative Foundation of Japan; Princess Takamatsu Cancer Research Fund; and the Uehara Memorial Foundation.

The costs of publication of this article were defrayed in part by the payment of page charges. This article must therefore be hereby marked *advertisement* in accordance with 18 U.S.C. Section 1734 solely to indicate this fact.

Received January 9, 2011; revised March 7, 2011; accepted March 15, 2011; published OnlineFirst March 23, 2011.

References

1. Morris SW, Kirstein MN, Valentine MB, Dittmer KG, Shapiro DN, Saltman DL, et al. Fusion of a kinase gene, ALK, to a nucleolar protein gene, NPM, in non-Hodgkin's lymphoma. Science 1994; 263:1281–4.
2. Shiota M, Fujimoto J, Semba T, Satoh H, Yamamoto T, Mori S. Hyperphosphorylation of a novel 80 kDa protein-tyrosine kinase similar to Ltk in a human Ki-1 lymphoma cell line, AMS3. Oncogene 1994;9:1567–74.
3. Lamant L, Dastugue N, Pulford K, Delsol G, Mariame B. A new fusion gene TPM3-ALK in anaplastic large cell lymphoma created by a (1;2)(q25;p23) translocation. Blood 1999;93:3088–95.
4. Meech SJ, McGavran L, Odom LF, Liang X, Meltesen L, Gump J, et al. Unusual childhood extramedullary hematologic malignancy with natural killer cell properties that contains tropomyosin 4–anaplastic lymphoma kinase gene fusion. Blood 2001;98:1209–16.
5. Colleoni GW, Bridge JA, Garicochea B, Liu J, Filippa DA, Ladanyi M. ATIC-ALK: A novel variant ALK gene fusion in anaplastic large cell lymphoma resulting from the recurrent cryptic chromosomal inversion, inv(2)(p23q35). Am J Pathol 2000;156:781–9.
6. Hernández L, Pinyol M, Hernández S, Beà S, Pulford K, Rosenwald A, et al. TRK-fused gene (TFG) is a new partner of ALK in anaplastic large cell lymphoma producing two structurally different TFG-ALK translocations. Blood 1999;94:3265–8.
7. Touriol C, Greenland C, Lamant L, Pulford K, Bernard F, Rousset T, et al. Further demonstration of the diversity of chromosomal changes involving 2p23 in ALK-positive lymphoma: 2 cases expressing ALK kinase fused to CLTCL (clathrin chain polypeptide-like). Blood 2000;95:3204–7.
8. Tort F, Pinyol M, Pulford K, Roncador G, Hernandez L, Nayach I, et al. Molecular characterization of a new ALK translocation involving moesin (MSN-ALK) in anaplastic large cell lymphoma. Lab Invest 2001;81:419–26.
9. Lamant L, Gascoyne RD, Duplantier MM, Armstrong F, Raghab A, Chhanabhai M, et al. Non-muscle myosin heavy chain (MYH9): a new partner fused to ALK in anaplastic large cell lymphoma. Genes Chromosomes Cancer 2003;37:427–32.
10. Cools J, Wlodarska I, Somers R, Mentens N, Pedeutour F, Maes B, et al. Identification of novel fusion partners of ALK, the anaplastic lymphoma kinase, in anaplastic large-cell lymphoma and inflammatory myofibroblastic tumor. Genes Chromosomes Cancer 2002;34: 354–62.
11. Lawrence B, Perez-Atayde A, Hibbard MK, Rubin BP, Dal Cin P, Pinkus JL, et al. TPM3-ALK and TPM4-ALK oncogenes in inflammatory myofibroblastic tumors. Am J Pathol 2000;157:377–84.
12. Bridge JA, Kanamori M, Ma Z, Pickering D, Hill DA, Lydiatt W, et al. Fusion of the ALK gene to the clathrin heavy chain gene, CLTC, in inflammatory myofibroblastic tumor. Am J Pathol 2001;159:411–5.
13. Ma Z, Hill DA, Collins MH, Morris SW, Sumegi J, Zhou M, et al. Fusion of ALK to the Ran-binding protein 2 (RANBP2) gene in inflammatory myofibroblastic tumor. Genes Chromosomes Cancer 2003;37:98–105.
14. Debiec-Rychter M, Marynen P, Hagemeijer A, Pauwels P. ALK-ATIC fusion in urinary bladder inflammatory myofibroblastic tumor. Genes Chromosomes Cancer 2003;38:187–90.
15. Panagopoulos I, Nilsson T, Domanski HA, Isaksson M, Lindblom P, Mertens F, et al. Fusion of the SEC31L1 and ALK genes in an inflammatory myofibroblastic tumor. Int J Cancer 2006;118:1181–6.
16. Delsol G, Lamant L, Mariamé B, Pulford K, Dastugue N, Brousset P, et al. A new subtype of large B-cell lymphoma expressing the ALK kinase and lacking the 2; 5 translocation. Blood 1997;89:1483–90.
17. Gascoyne RD, Lamant L, Martin-Subero JI, Lestou VS, Harris NL, Müller-Hermelink HK, et al. ALK-positive diffuse large B-cell lymphoma is associated with Clathrin-ALK rearrangements: report of 6 cases. Blood 2003;102:2568–73.
18. Van Roosbroeck K, Cools J, Dierickx D, Thomas J, Vandenberghe P, Stul M, et al. ALK-positive large B-cell lymphomas with cryptic SEC31A-ALK and NPM1-ALK fusions. Haematologica 2010;95: 509–13.
19. Takeuchi K, Soda M, Togashi Y, Ota Y, Sekiguchi Y, Hatano S, et al. Identification of a novel fusion, SQSTM1-ALK, in ALK-positive large B-cell lymphoma. Haematologica 2010.
20. Soda M, Choi YL, Enomoto M, Takada S, Yamashita Y, Ishikawa S, et al. Identification of the transforming EML4-ALK fusion gene in non-small-cell lung cancer. Nature 2007;448:561–6.
21. Takeuchi K, Choi YL, Togashi Y, Soda M, Hatano S, Inamura K, et al. KIF5B-ALK, a novel fusion oncokinase identified by an immunohistochemistry-based diagnostic system for ALK-positive lung cancer. Clin Cancer Res 2009;15:3143–9.
22. Chan JK, Lamant L, Algar E, Delsol G, Tsang WY, Lee KC, et al. ALK+ histiocytosis: a novel type of systemic histiocytic proliferative disorder of early infancy. Blood 2008;112:2965–8.
23. Du XL, Hu H, Lin DC, Xia SH, Shen XM, Zhang Y, et al. Proteomic profiling of proteins dysregulted in Chinese esophageal squamous cell carcinoma. J Mol Med 2007;85:863–75.
24. Jazii FR, Najafi Z, Malekzadeh R, Conrads TP, Ziaee AA, Abnet C, et al. Identification of squamous cell carcinoma associated proteins by proteomics and loss of beta tropomyosin expression in esophageal cancer. World J Gastroenterol 2006;12:7104–12.
25. Rikova K, Guo A, Zeng Q, Possemato A, Yu J, Haack H, et al. Global survey of phosphotyrosine signaling identifies oncogenic kinases in lung cancer. Cell 2007;131:1190–203.
26. Lin E, Li L, Guan Y, Soriano R, Rivers CS, Mohan S, et al. Exon array profiling detects EML4-ALK fusion in breast, colorectal, and non-small cell lung cancers. Mol Cancer Res 2009;7:1466–76.
27. Chiarle R, Voena C, Ambrogio C, Piva R, Inghirami G. The anaplastic lymphoma kinase in the pathogenesis of cancer. Nat Rev Cancer 2008;8:11–23.
28. Kwak EL, Bang YJ, Camidge DR, Shaw AT, Solomon B, Maki RG, et al. Anaplastic lymphoma kinase inhibition in non-small-cell lung cancer. N Engl J Med 2010;363:1693–703.
29. Butrynski JE, D'Adamo DR, Hornick JL, Dal Cin P, Antonescu CR, Jhanwar SC, et al. Crizotinib in ALK-rearranged inflammatory myofibroblastic tumor. N Engl J Med 2010;363:1727–33.
30. Falini B, Bigerna B, Fizzotti M, Pulford K, Pileri SA, Delsol G, et al. ALK expression defines a distinct group of T/null lymphomas ("ALK lymphomas") with a wide morphological spectrum. Am J Pathol 1998;153:875–86.
31. Sakairi Y, Nakajima T, Yasufuku K, Ikebe D, Kageyama H, Soda M, et al. EML4-ALK fusion gene assessment using metastatic lymph node samples obtained by endobronchial ultrasound-guided transbronchial needle aspiration. Clin Cancer Res 2010;16:4938–45.
32. Nakajima T, Kimura H, Takeuchi K, Soda M, Mano H, Yasufuku K, et al. Treatment of lung cancer with an ALK inhibitor after EML4-ALK fusion gene detection using endobronchial ultrasound-guided transbronchial needle aspiration. J Thorac Oncol 2010;5:2041–3.
33. Jokoji R, Yamasaki T, Minami S, Komuta K, Sakamaki Y, Takeuchi K, et al. Combination of morphological feature analysis and immunohistochemistry is useful for screening of EML4-ALK-positive lung adenocarcinoma. J Clin Pathol 2010;63:1066–70.
34. Mino-Kenudson M, Chirieac LR, Law K, Hornick JL, Lindeman N, Mark EJ, et al. A novel, highly sensitive antibody allows for the routine detection of ALK-rearranged lung adenocarcinomas by standard immunohistochemistry. Clin Cancer Res 2010;16:1561–71.
35. Martelli MP, Sozzi G, Hernandez L, Pettirossi V, Navarro A, Conte D, et al. EML4-ALK rearrangement in non-small cell lung cancer and non-tumor lung tissues. Am J Pathol 2009;174:661–70.
36. Shiota M, Nakamura S, Ichinohasama R, Abe M, Akagi T, Takeshita M, et al. Anaplastic large cell lymphomas expressing the novel chimeric protein p80NPM/ALK: a distinct clinicopathologic entity. Blood 1995;86:1954–60.
37. Takeuchi K, Choi YL, Soda M, Inamura K, Togashi Y, Hatano S, et al. Multiplex reverse transcription-PCR screening for EML4-ALK fusion transcripts. Clin Cancer Res 2008;14:6618–24.
38. Choi YL, Takeuchi K, Soda M, Inamura K, Togashi Y, Hatano S, et al. Identification of novel isoforms of the EML4-ALK transforming gene in non-small cell lung cancer. Cancer Res 2008;68:4971–6.

39. Onishi M, Kinoshita S, Morikawa Y, Shibuya A, Phillips J, Lanier LL, et al. Applications of retrovirus-mediated expression cloning. Exp Hematol 1996;24:324–9.
40. Pillay K, Govender D, Chetty R. ALK protein expression in rhabdomyosarcomas. Histopathology 2002;41:461–7.
41. Passoni L, Longo L, Collini P, Coluccia AM, Bozzi F, Podda M, et al. Mutation-independent anaplastic lymphoma kinase overexpression in poor prognosis neuroblastoma patients. Cancer Res 2009;69:7338–46.
42. Travis WD, Elisabeth B, Muller-Hermelink HK, Harris CC, editors. Pathology and Genetics of Tumours of the Lung, Pleural, Thymus and Heart. Lyon: IARC Press; 2004.
43. Kriajevska M, Fischer-Larsen M, Moertz E, Vorm O, Tulchinsky E, Grigorian M, et al. Liprin beta 1, a member of the family of LAR transmembrane tyrosine phosphatase-interacting proteins, is a new target for the metastasis-associated protein S100A4 (Mts1). J Biol Chem 2002;277:5229–35.
44. Norrmén C, Vandevelde W, Ny A, Saharinen P, Gentile M, Haraldsen G, et al. Liprin (beta)1 is highly expressed in lymphatic vasculature and is important for lymphatic vessel integrity. Blood 2010;115:906–9.
45. Debelenko LV, Raimondi SC, Daw N, Shivakumar BR, Huang D, Nelson M, et al. Renal cell carcinoma with novel VCL-ALK fusion: new representative of ALK-associated tumor spectrum. Mod Pathol 2010.
46. Marino-Enriquez A, Ou WB, Weldon CB, Fletcher JA, Perez-Atayde AR. ALK rearrangement in sickle cell trait-associated renal medullary carcinoma. Genes Chromosomes Cancer 2011;50:146–53.

OPEN ACCESS Freely available online

PLoS one

KLC1-ALK: A Novel Fusion in Lung Cancer Identified Using a Formalin-Fixed Paraffin-Embedded Tissue Only

Yuki Togashi[1,2], Manabu Soda[3], Seiji Sakata[1], Emiko Sugawara[1,4], Satoko Hatano[1,2], Reimi Asaka[1,2], Takashi Nakajima[5], Hiroyuki Mano[3,6], Kengo Takeuchi[1,2]*

1 Pathology Project for Molecular Targets, The Cancer Institute, Japanese Foundation for Cancer Research, Tokyo, Japan, **2** Division of Pathology, The Cancer Institute, Japanese Foundation for Cancer Research, Tokyo, Japan, **3** Division of Functional Genomics, Jichi Medical University, Tochigi, Japan, **4** Department of Comprehensive Pathology, Graduate School, Tokyo Medical and Dental University, Tokyo, Japan, **5** Division of Diagnostic Pathology, Shizuoka Cancer Center, Nagaizumi, Shizuoka, Japan, **6** Department of Medical Genomics, Graduate School of Medicine, University of Tokyo, Tokyo, Japan

Abstract

The promising results of anaplastic lymphoma kinase (ALK) inhibitors have changed the significance of ALK fusions in several types of cancer. These fusions are no longer mere research targets or diagnostic markers, but they are now directly linked to the therapeutic benefit of patients. However, most available tumor tissues in clinical settings are formalin-fixed and paraffin-embedded (FFPE), and this significantly limits detailed genetic studies in many clinical cases. Although recent technical improvements have allowed the analysis of some known mutations in FFPE tissues, identifying unknown fusion genes by using only FFPE tissues remains difficult. We developed a 5′-rapid amplification of cDNA ends-based system optimized for FFPE tissues and evaluated this system on a lung cancer tissue with *ALK* rearrangement and without the 2 known ALK fusions EML4-ALK and KIF5B-ALK. With this system, we successfully identified a novel ALK fusion, KLC1-ALK. The result was confirmed by reverse transcription-polymerase chain reaction and fluorescence *in situ* hybridization. Then, we synthesized the putative full-length cDNA of *KLC1-ALK* and demonstrated the transforming potential of the fusion kinase with assays using mouse 3T3 cells. To the best of our knowledge, KLC1-ALK is the first novel oncogenic fusion identified using only FFPE tissues. This finding will broaden the potential value of archival FFPE tissues and provide further biological and clinical insights into ALK-positive lung cancer.

Citation: Togashi Y, Soda M, Sakata S, Sugawara E, Hatano S, et al. (2012) KLC1-ALK: A Novel Fusion in Lung Cancer Identified Using a Formalin-Fixed Paraffin-Embedded Tissue Only. PLoS ONE 7(2): e31323. doi:10.1371/journal.pone.0031323

Editor: Anthony W.I. Lo, The Chinese University of Hong Kong, Hong Kong

Received October 17, 2011; **Accepted** January 5, 2012; **Published** February 8, 2012

Funding: This work was supported in part by Grants-in-Aid for Scientific Research from the Ministry of Education, Culture, Sports, Science, and Technology of Japan as well as by grants from the Japan Society for the Promotion of Science; the Ministry of Health, Labor, and Welfare of Japan; the Vehicle Racing Commemorative Foundation of Japan; the Princess Takamatsu Cancer Research Fund; and the Uehara Memorial Foundation. The funders had no role in study design, data collection and analysis, decision to publish, or preparation of the manuscript.

Competing Interests: The authors have declared that no competing interests exist.

* E-mail: kentakeuchi-tky@umin.net

Introduction

Anaplastic lymphoma kinase (ALK) is a receptor tyrosine kinase that was discovered in anaplastic large-cell lymphoma (ALCL) in the form of a fusion protein, NPM-ALK [1,2]. The formation of a fusion protein with a partner through chromosomal translocations is the most common mechanism of ALK overexpression and ALK kinase domain activation. Recent promising results of clinical trials with an ALK inhibitor, crizotinib, have changed the significance of ALK fusions in lung cancer [3,4,5,6], inflammatory myofibroblastic tumors (IMTs) [7], and ALCL [8]. ALK fusions are no longer mere research targets or diagnostic markers and are now directly linked to the therapeutic benefit of patients.

In lung cancer, 3 fusion partners of ALK have been reported—EML4, TFG, and KIF5B—although the presence of TFG-ALK in lung cancer has not yet been proven with histopathological evidence [9,10,11]. In addition to lung cancer, ALK has further been found to generate fusions in ALCL (fused to NPM, TPM3, TPM4, ATIC, TFG, CLTC, MSN, MYH9, or ALO17) [1,2,12,13,14,15,16,17,18,19], IMT (TPM3, TPM4, CLTC, CARS, RANBP2, ATIC, or SEC31A) [19,20,21,22,23,24], ALK-positive large B-cell lymphoma (CLTC, NPM, SEC31A, or SQSTM1) [25,26,27,28], and renal cancer (VCL, TPM3 or EML4) (Table 1) [29,30]. In addition to TFG-ALK in lung cancer, some ALK fusions have been reported without histopathological evidence: TPM4-ALK in esophageal squamous cell carcinoma [31,32] and EML4-ALK in colon and breast carcinomas [33].

Anti-ALK immunohistochemistry played an important role in identifying these ALK fusion partners. Several ALK fusions exhibit a characteristic staining pattern in anti-ALK immunohistochemistry because the subcellular localization of ALK fusion proteins depends on the fusion partner. For example, NPM-ALK, which is the most common fusion in ALK-positive ALCL (85%), exhibits a nuclear and cytoplasmic staining pattern because the heterodimer of NPM and NPM-ALK localizes in the nucleus and the homodimer of NPM-ALK in the cytoplasm; CLTC-ALK exhibits a cytoplasmic granular pattern because it localizes in the small vesicles. If a tumor exhibits an unrecognized anti-ALK staining pattern, the patient may have a novel fusion partner. In addition to the difference in subcellular localization, the difference in staining intensity is a key to identifying novel partners. EML4-ALK is hardly stained by conventional anti-ALK immunohistochemistry [11,34]. To overcome this limitation, we developed the intercalated antibody-enhanced polymer (iAEP) method, which moderately increases

Table 1. ALK fusion partners.

Reported year	Partner	Locus	ALK+ALCL	ALK+LBCL	IMT	NSCLC	RCC
1994	NPM	5q35.1	+	+			
1999	TPM3	1p23	+		+		+
1999	TFG	3q12.2	+			+*	
2000	ATIC	2q35	+		+		
2000	TPM4	19p13	+		+		
2001	CLTC	17q23	+	+	+		
2001	MSN	Xp11.1	+				
2002	ALO17	17q25.3	+				
2003	MYH9	22q13.1	+				
2003	RANBP2	2q13			+		
2003	CARS	11p15			+		
2006	SEC31A	4q41		+	+		
2007	EML4	2p21				+	+
2009	KIF5B	10p11.22				+	
2011	SQSTM1	5q35.3		+			
2011	PPFIBP1	12p11			+		
2011	VCL	10q22.2					+
Present study	KLC1	14q32.1				+	

*Histopathological evidence is lacking. Abbreviations: ALCL, anaplastic large cell lymphoma; LBCL, large B-cell lymphoma; IMT, inflammatory myofibroblastic tumor; NSCLC, non-small cell lung carcinoma; RCC, renal cell carcinoma.

doi:10.1371/journal.pone.0031323.t001

sensitivity in the immunohistochemical detection system, and EML4-ALK was consistently stained with this method [11]. This indicated that a tumor that is positively immunostained for ALK only by a sensitive immunohistochemistry method but not by conventional methods may harbor a novel ALK fusion. Based on this hypothesis, we successfully identified PPFIBP1-ALK in 2 IMT cases that were positive in anti-ALK immunohistochemistry only when stained by the iAEP method [35].

Anti-ALK immunohistochemistry may thus be useful to detect candidate tumors for a novel ALK fusion. However, to identify the fusion partner, other molecular techniques are usually required such as 5′-rapid amplification of cDNA ends (5′-RACE) or inverse reverse-transcription polymerase chain reaction (RT-PCR). To the best of our knowledge, no novel oncogenic fusions have been discovered using formalin-fixed paraffin-embedded (FFPE) tissues only because nucleic acids extracted from FFPE tissues are severely degraded during the fixation process. In the present study, we developed a 5′-RACE method optimized for *ALK* fusion partner detection that was applicable to FFPE tissues and identified a novel fusion, kinesin light chain 1 (KLC1)-ALK, in lung cancer by using only an FFPE tissue.

Methods

Materials

A FFPE tissue block of pulmonary adenocarcinoma in situ, nonmucinous (formerly called bronchioloalveolar carcinoma) [36], which was excised from a 47-year-old female patient was used [37]. This carcinoma was negative for EML4-ALK and KIF5B-ALK, although the presence of *ALK* rearrangement was confirmed by anti-ALK iAEP immunohistochemistry and a split fluorescence in situ hybridization (FISH) assay for ALK (hereafter referred to as the unknown ALK fusion-positive case) (Figure 1) [37]. Two FFPE tissue blocks of ALK-positive tumor cases were also employed, for which the presence of EML4-ALK or KIF5B-ALK had already been confirmed. Total RNA was extracted from each FFPE tissue with the use of the RecoverAll™ Total Nucleic Acid Isolation Kit for FFPE (Applied Biosystems Japan, Tokyo, Japan). The ages of the 3 FFPE blocks used (time from FFPE tissue production to RNA extraction) were 65, 40, and 51 months for the unknown ALK fusion-positive case, EML4-ALK, and KIF5B-ALK, respectively. Written informed consent was obtained from each patient. The study was approved by the institutional review board of the Shizuoka Cancer Center (approval ID 22-J132-22-1) and the Japanese Foundation for Cancer Research (approval ID 2010-1011).

Modified 5′-RACE for ALK fusions applicable to FFPE tissues

5′-RACE was performed with the SMARTer RACE cDNA Amplification Kit (Clontech) according to the manufacturer's instruction with minor modifications. In brief, instead of the primers included in the kit, ALK-3242R (5′-CTCAGCTTG-TACTCAGGGC-3′) was used for cDNA synthesis. The cDNA was subjected to 5′-RACE PCR using PrimeSTAR HS DNA Polymerase (TaKaRa) and the following primers: Universal Primer A Mix of the kit and ALK-3206R (5′-ATGGCTTG-CAGCTCCTGGTGCTT-3′). The PCR condition consisted of 5 cycles at 94°C for 30 s and 72°C for 3 min; 5 cycles at 94°C for 30 s, 70°C for 30 s, and 72°C for 3 min; and 30 cycles at 94°C for 30 s, 68°C for 30 s, and 72°C for 3 min.

FISH

FISH analysis of fusion genes was performed with DNA probes for KLC1 and ALK. Unstained sections (4-μm thick) were subjected to hybridization with an ALK-split probe set (Dako, Tokyo, Japan) or with bacterial artificial chromosome (BAC) clone-derived probes for ALK (RP11-984I21 and RP11-62B19)

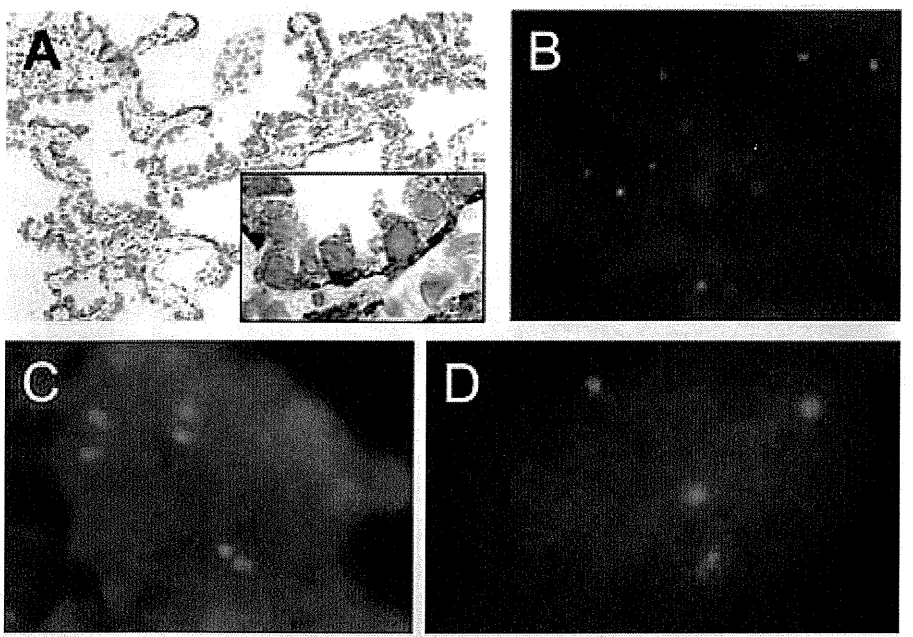

Figure 1. ALK-rearranged lung adenocarcinoma without EML4-ALK and KIF5B-ALK. Panel A shows the results of anti-ALK immunohistochemistry with the iAEP method on pulmonary adenocarcinoma in situ, nonmucinous. The staining pattern was diffusely cytoplasmic. The basal side of tumor cells was more strongly stained, indicating an uneven subcellular localization of KLC1-ALK protein. FISH analyses revealed that this case was positive in the split assay for *ALK* (Panel B: individual 5′- and 3′-signals are observed) and negative in *EML4-ALK* and *KIF5B-ALK* fusion assays (Panel C: *EML4*, red; *ALK*, green; Panel D: *KIF5B*, green; *ALK*, red).
doi:10.1371/journal.pone.0031323.g001

and KLC1 (RP11-186F6). Hybridized slides were then stained with DAPI and examined using a BX51 fluorescence microscope (Olympus, Tokyo, Japan).

Synthesis of the putative cDNA of *KLC1-ALK*

Two independent PCRs were performed using cDNA synthesized from a tumor tissue expressing KIF5B-ALK with the following primer sets: KLC1-NheI-M (5′-GCGCTAGCGAATGTATGACAACATGTCCAC-3′) and KLC1-bpR (5′-GTGCTTCCGGCGGTACACATCTACAGAACCAAACTC-3′), and ALK-bpF (5′-GGGAGTTTGGTTCTGTAGATGTGTACCGCCGGAAGC-3′) and ALK-EcoRI (5′-GATAGAATTCTCAGGGCCCAGGCT-3′). Then, the second PCR was performed using a 1/100 dilution of a mixture of the first PCR products as a template with the KLC1-NheI-M and ALK-EcoRI primers (Figure 2).

Transformation assay for *KLC1-ALK*

Analysis of the transforming activity of kinase fusions was performed as described previously [9,38,39]. A pMXS-based expression plasmid for each fusion was used to generate recombinant ecotropic retroviruses [40], which were then used individually to infect mouse 3T3 fibroblasts. The formation of transformed foci was evaluated after culturing the cells for 4 days. The same set of 3T3 cells was injected subcutaneously into nu/nu mice, and tumor formation was examined after 14 days. The animal experiments were approved by the animal ethics committee of Jichi Medical University (approval ID 1135).

Results

Identification of *KLC1-ALK* as a novel *ALK* fusion gene

Our modified 5′-RACE faithfully isolated cDNA fragments for *EML4-ALK* or *KIF5B-ALK* from known ALK- positive tumors (Supplementary Figure S1A and B). We then attempted to isolate cDNA fragments encompassing the fusion points from the unknown ALK fusion-positive case. Nucleotide sequencing of such 5′-RACE products revealed that 2 of 10 clones contained the 3′-terminus of exon 9 of *KLC1* (ENST00000348520) fused to the first nucleotide of exon 20 of *ALK* (ENST00000389048), indicating the presence of a novel fusion between *KLC1* and *ALK*. As this rearrangement constituted an in-frame fusion between the 2 genes, the full-length *KLC1-ALK* cDNA probably produces a protein of 984 amino acids containing an amino-terminal two-thirds of KLC1 and an intracellular region of ALK (Figure 3A). RT-PCR-mediated isolation of a fusion point successfully confirmed the in-frame fusion between the 2 messages (Figure 3A and B). Further, to confirm the genomic rearrangement responsible for the fusion, a fusion FISH assay was performed (Figure 3C). These results were consistent with the presence of t(2;14)(p23;q32.3), leading to the generation of *KLC1-ALK*.

Transforming potential of *KLC1-ALK*

The putative full-length cDNA of *KLC1-ALK* was synthesized from the frozen tissue with KIF5B-ALK fusion expression (Figure 2, Supplementary Figure S2), and was used to generate a recombinant retrovirus expressing the fusion protein with an amino-terminal FLAG epitope tag. Infection of 3T3 cells with the virus expressing KLC1-ALK readily produced multiple transformed foci in culture and subcutaneous tumors in a nude mouse tumorigenicity assay (Figure 4), confirming the potent transforming ability of KLC1-ALK.

Discussion

Here, by analyzing the FFPE tissues only, we successfully discovered a novel ALK fusion, KLC1-ALK. While snap-frozen materials sampled from biopsied or surgically removed specimens

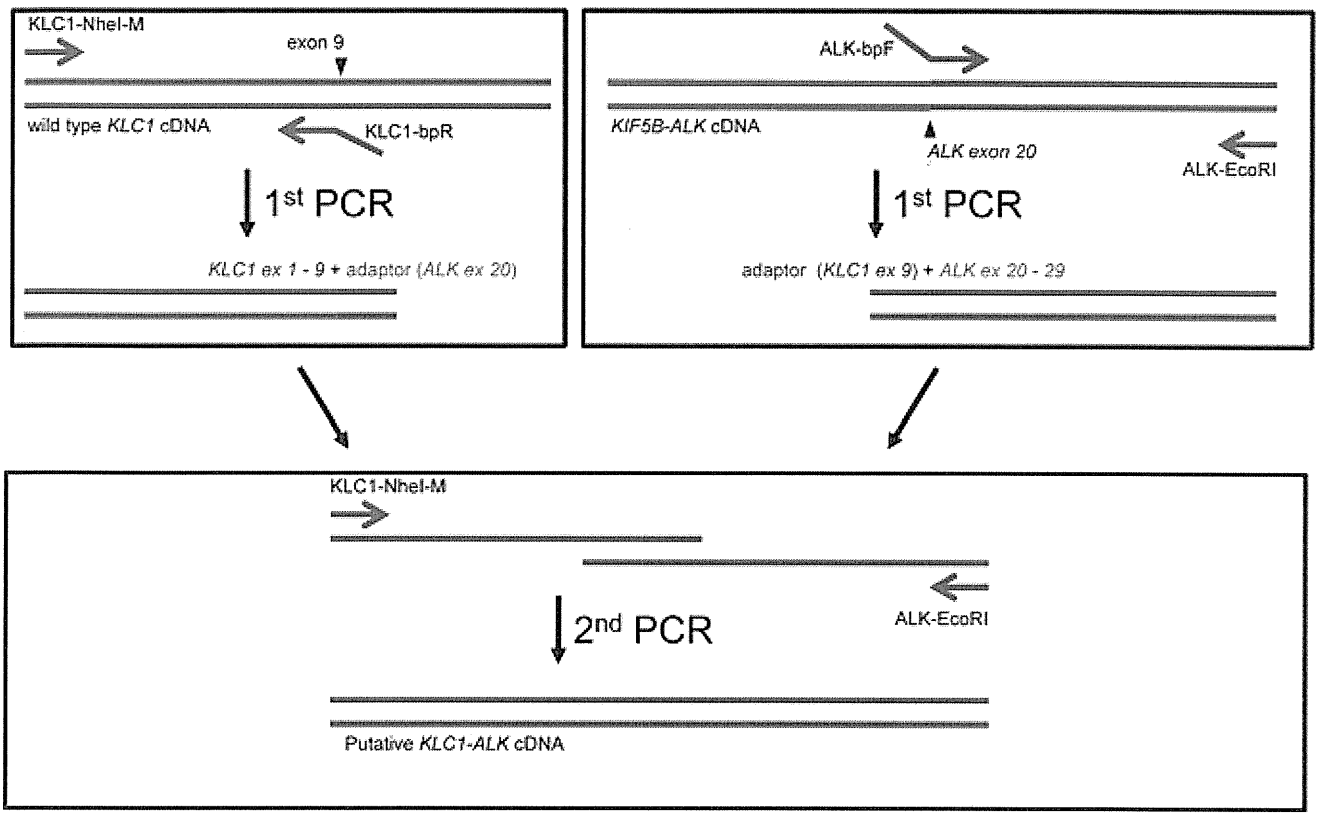

Figure 2. Synthesis of the putative KLC1-ALK full-length cDNA. Two first-round PCRs were performed separately using cDNA synthesized from a tumor tissue expressing KIF5B-ALK with the following primer sets: KLC1-NheI-M and KLC1-bpR, and ALK-bpF and ALK-EcoRI. KLC1-bpR and ALK-bpF had sequences downstream of the ALK break point (exon 20) and upstream of the KLC1 break point (exon 9) as adopter sequences, respectively. Then, the second PCR was performed using a 1/100 dilution of the mixture of the first PCR products as a template with primers KLC1-NheI-M and ALK-EcoRI. The first PCR products were annealed, extended with each other, and then amplified with the primers.
doi:10.1371/journal.pone.0031323.g002

can be used for various types of molecular analyses, they are not routinely sampled in most clinical settings. In contrast, FFPE specimens are usually produced, and histopathology diagnostic archives are an extremely large resource of FFPE tissues in ordinary diagnostic pathology laboratories. However, DNA and RNA extracted from FFPE tissues are severely degraded during formalin fixation and are usually not suitable for assays that need long DNA/RNA of high quality. Recent technical advances have allowed some analyses for known point mutations and known fusion genes, but it is still difficult to identify an unrecognized gene aberration using only an FFPE tissue.

In most *ALK* fusions, the break point of *ALK* is located within intron 19, and the fusion point in mRNA is typically the first nucleotide of exon 20. Therefore, if the primers for 5′-RACE are placed immediately downstream of the first nucleotide of *ALK* exon 20, such 5′-RACE may successfully isolate PCR products containing the partner gene sequence even using FFPE tissues. Based on this hypothesis, we established a 5′-RACE system for *ALK* fusions optimized for FFPE tissues. With this system, we identified a novel *ALK* fusion, *KLC1-ALK*. To the best of our knowledge, this is the first novel oncogenic fusion identified using only an FFPE tissue.

Caution, however, is needed. In some rare cases with *ALK* fusion, the break point of *ALK* fusion mRNA may not be at the 5′-end of exon 20. For example, in variant 4 of *EML4-ALK*, exon 14 of *EML4* is fused to an unknown sequence of 11 bp, which in turn is connected to nucleotide 50 of *ALK* exon 20 (E14;ins11;del49A20) [38]. Our 5′-RACE system would not work on such a case because the reverse primer ALK-3206R corresponds to nucleotides 12–34 of *ALK* exon 20. Therefore, if our modified 5′-RACE fails to isolate fusion cDNAs from cases with a confirmed ALK rearrangement, other primer settings may be attempted.

Kinesin is a heterotetramer of 2 kinesin heavy chains and 2 kinesin light chains, and it moves on the microtubules towards their plus ends carrying various cargos. The heavy chains harbor the motor activity, whereas the light chains play roles in cargo binding and in modulating the activity and subcellular localization of the heavy chains. KLC1 binds to the kinesin heavy chains with an N-terminal domain and to various cargos via the tetratricopeptide repeat domains [41,42]. Of the 3 histopathologically confirmed ALK fusion partners in lung cancer, EML4 colocalizes with microtubules and may contribute to the stabilization of microtubules [43], KIF5B moves on the microtubules as a kinesin heavy chain [44], and KLC1 binds to kinesin heavy chains as a kinesin light chain. Therefore, it is interesting that all the 3 ALK fusions in lung cancer are likely to colocalize with microtubules.

The most frequent ALK fusion in lung cancer is EML4-ALK (4–7%) [9,38], and the second is KIF5B-ALK (0.5%) [11]. One case with TFG-ALK is reported [10]. KLC1-ALK may be rare but exists in lung adenocarcinoma, and the patients with this fusion are highly likely to benefit from ALK inhibitor therapy as do patients with other ALK fusions. The incidence may be low, but the significance of this fusion is very high from the perspective

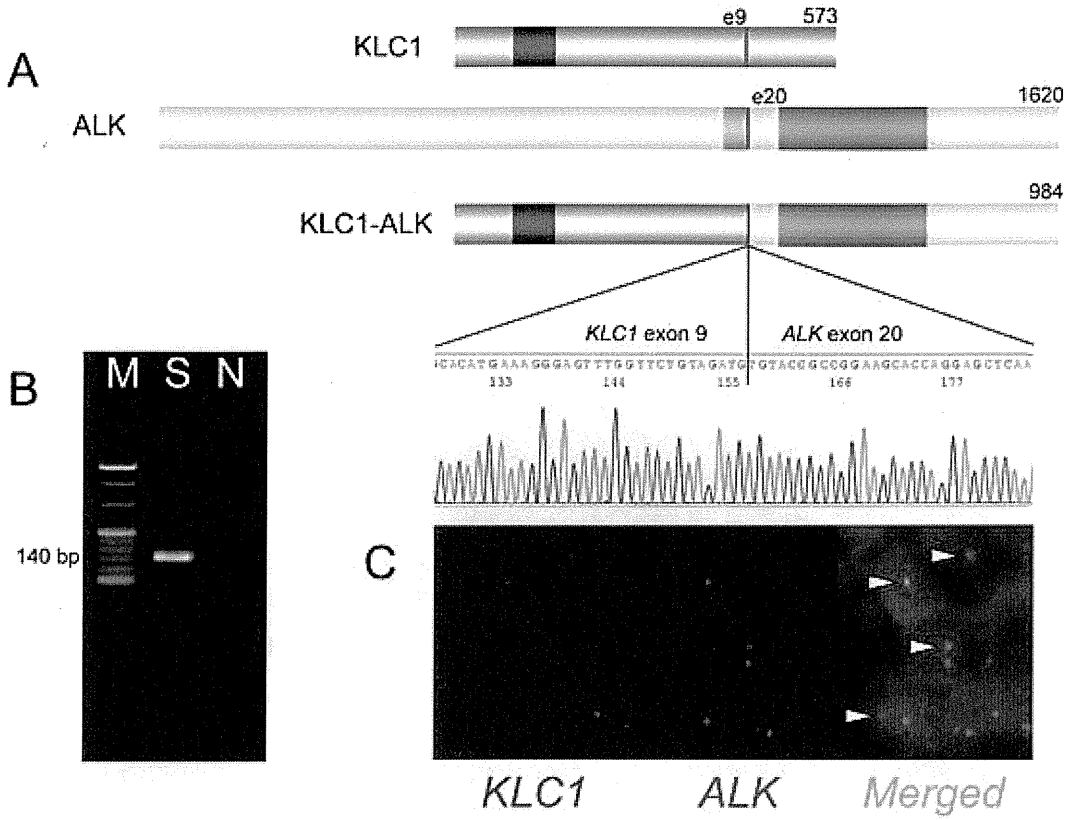

Figure 3. Identification of KLC1-ALK. Panel A shows the schematic structure of KLC1, ALK, and KLC1-ALK proteins and the cDNA sequence around the fusion point. Dark blue, orange, and red parts represent coiled-coil, transmembrane, and kinase domains, respectively. The break point exons and the number of amino acids are indicated. KLC1-ALK-specific RT-PCR using RNA extracted from the FFPE tissue of the unknown ALK fusion-positive case amplified a fragment of the expected product size (140 bp, Panel B) with the consistent fusion sequence (Panel A). A fusion FISH assay for *KLC1-ALK* revealed a fusion signal (yellow) in multiple tumor cells (Panel C). M, marker (100-bp ladder); S, sample (the unknown ALK fusion-positive case); N, no template control.
doi:10.1371/journal.pone.0031323.g003

of a tailor-made therapeutic option for the patient. Another important point is that KLC1-ALK was found in adenocarcinoma in situ, nonmucinous (formerly called bronchioloalveolar carcinoma, BAC). BAC is recognized to rarely harbor ALK fusions, although a small number of BAC cases has been examined for ALK fusion compared with invasive adenocarcinoma. It would be interesting from a pathobiological perspective to examine a large-scale cohort of BAC and other premalignant conditions for ALK fusion.

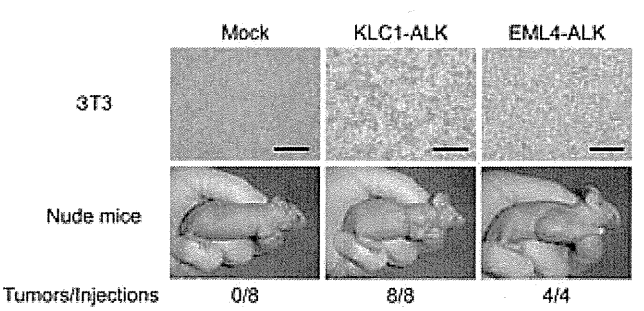

Figure 4. Transforming potential of KLC1-ALK. Upper panels: Mouse 3T3 fibroblasts were infected with retroviruses encoding KLC1-ALK or EML4-ALK or with the corresponding empty virus (Mock). The cells were photographed after 4 days of culture. Scale bar, 1 mm. Lower panels: Nude mice were injected subcutaneously with the corresponding 3T3 cells, and tumor formation was examined after 14 days. The number of tumors formed per injections is indicated at the bottom.
doi:10.1371/journal.pone.0031323.g004

There are 3 methods for the detection of ALK fusions: RT-PCR, ALK split FISH, and high-sensitivity anti-ALK immunohistochemistry. For RT-PCR, the 5′ partner gene must be known. Our findings in this study identified one more partner gene that should be targeted in ALK-fusion detection using RT-PCR in lung cancer. The other 2 methods can detect all ALK fusions regardless of fusion partner and, therefore, are suitable for ALK-fusion screening. In other words, these 2 methods cannot identify the fusion partner and need to be succeeded by partner-specific RT-PCR and/or fusion FISH for this purpose. If it is revealed that the partner gene in the tested case is unknown, a novel partner gene is highly likely to be discovered, as was shown in the present study. In fact, using high-sensitivity anti-ALK immunohistochemistry (iAEP method) as screening, we have identified several novel ALK fusions in various types of cancers including lung adenocarcinoma [11], lymphoma [28], sarcoma [35], and renal cell carcinoma [30].

Many efficient tools have been established for the detection of ALK fusion-positive cases using FFPE tissues, including anti-ALK immunohistochemistry and FISH. Our findings will further expand the potential value of archival FFPE tissues and provide further biological and clinical insights into ALK-positive cancers in the forthcoming era of ALK inhibitor therapy.

Supporting Information

Figure S1 5′-RACE products using FFPE tissues. Our modified 5′-RACE faithfully isolated cDNA fragments for *EML4-ALK* (A) or *KIF5B-ALK* (B) from known ALK- positive tumors.
(TIF)

Figure S2 Putative cDNA sequence of KLC1-ALK. The putative full-length cDNA of *KLC1-ALK* was synthesized from the frozen tissue with KIF5B-ALK fusion expression.
(PDF)

References

1. Morris SW, Kirstein MN, Valentine MB, Dittmer KG, Shapiro DN, et al. (1994) Fusion of a kinase gene, ALK, to a nucleolar protein gene, NPM, in non-Hodgkin's lymphoma. Science 263: 1281–1284.
2. Shiota M, Fujimoto J, Semba T, Satoh H, Yamamoto T, et al. (1994) Hyperphosphorylation of a novel 80 kDa protein-tyrosine kinase similar to Ltk in a human Ki-1 lymphoma cell line, AMS3. Oncogene 9: 1567–1574.
3. Kwak EL, Bang YJ, Camidge DR, Shaw AT, Solomon B, et al. (2010) Anaplastic lymphoma kinase inhibition in non-small-cell lung cancer. N Engl J Med 363: 1693–1703.
4. Kimura H, Nakajima T, Takeuchi K, Soda M, Mano H, et al. (2011) ALK fusion gene positive lung cancer and 3 cases treated with an inhibitor for ALK kinase activity. Lung Cancer.
5. Kijima T, Takeuchi K, Tetsumoto S, Shimada K, Takahashi R, et al. (2011) Favorable response to crizotinib in three patients with echinoderm microtubule-associated protein-like 4-anaplastic lymphoma kinase fusion-type oncogene-positive non-small cell lung cancer. Cancer Sci 102: 1602–1604.
6. Nakajima T, Kimura H, Takeuchi K, Soda M, Mano H, et al. (2010) Treatment of Lung Cancer with an ALK Inhibitor After EML4-ALK Fusion Gene Detection Using Endobronchial Ultrasound-Guided Transbronchial Needle Aspiration. J Thorac Oncol 5: 2041–2043.
7. Butrynski JE, D'Adamo DR, Hornick JL, Dal Cin P, Antonescu CR, et al. (2010) Crizotinib in ALK-rearranged inflammatory myofibroblastic tumor. N Engl J Med 363: 1727–1733.
8. Gambacorti-Passerini C, Messa C, Pogliani EM (2011) Crizotinib in anaplastic large-cell lymphoma. N Engl J Med 364: 775–776.
9. Soda M, Choi YL, Enomoto M, Takada S, Yamashita Y, et al. (2007) Identification of the transforming EML4-ALK fusion gene in non-small-cell lung cancer. Nature 448: 561–566.
10. Rikova K, Guo A, Zeng Q, Possemato A, Yu J, et al. (2007) Global survey of phosphotyrosine signaling identifies oncogenic kinases in lung cancer. Cell 131: 1190–1203.
11. Takeuchi K, Choi YL, Togashi Y, Soda M, Hatano S, et al. (2009) KIF5B-ALK, a novel fusion oncokinase identified by an immunohistochemistry-based diagnostic system for ALK-positive lung cancer. Clin Cancer Res 15: 3143–3149.
12. Lamant L, Dastugue N, Pulford K, Delsol G, Mariame B (1999) A new fusion gene TPM3-ALK in anaplastic large cell lymphoma created by a (1;2)(q25;p23) translocation. Blood 93: 3088–3095.
13. Meech SJ, McGavran L, Odom LF, Liang X, Meltesen L, et al. (2001) Unusual childhood extramedullary hematologic malignancy with natural killer cell properties that contains tropomyosin 4–anaplastic lymphoma kinase gene fusion. Blood 98: 1209–1216.
14. Colleoni GW, Bridge JA, Garicochea B, Liu J, Filippa DA, et al. (2000) ATIC-ALK: A novel variant ALK gene fusion in anaplastic large cell lymphoma resulting from the recurrent cryptic chromosomal inversion, inv(2)(p23q35). Am J Pathol 156: 781–789.
15. Hernandez L, Pinyol M, Hernandez S, Bea S, Pulford K, et al. (1999) TRK-fused gene (TFG) is a new partner of ALK in anaplastic large cell lymphoma producing two structurally different TFG-ALK translocations. Blood 94: 3265–3268.
16. Touriol C, Greenland C, Lamant L, Pulford K, Bernard F, et al. (2000) Further demonstration of the diversity of chromosomal changes involving 2p23 in ALK-positive lymphoma: 2 cases expressing ALK kinase fused to CLTCL (clathrin chain polypeptide-like). Blood 95: 3204–3207.
17. Tort F, Pinyol M, Pulford K, Roncador G, Hernandez L, et al. (2001) Molecular characterization of a new ALK translocation involving moesin (MSN-ALK) in anaplastic large cell lymphoma. Lab Invest 81: 419–426.
18. Lamant L, Gascoyne RD, Duplantier MM, Armstrong F, Raghab A, et al. (2003) Non-muscle myosin heavy chain (MYH9): a new partner fused to ALK in anaplastic large cell lymphoma. Genes Chromosomes Cancer 37: 427–432.
19. Cools J, Wlodarska I, Somers R, Mentens N, Pedeutour F, et al. (2002) Identification of novel fusion partners of ALK, the anaplastic lymphoma kinase, in anaplastic large-cell lymphoma and inflammatory myofibroblastic tumor. Genes Chromosomes Cancer 34: 354–362.
20. Lawrence B, Perez-Atayde A, Hibbard MK, Rubin BP, Dal Cin P, et al. (2000) TPM3-ALK and TPM4-ALK oncogenes in inflammatory myofibroblastic tumors. Am J Pathol 157: 377–384.

Acknowledgments

We thank Mr. Motoyoshi Iwakoshi, Ms. Keiko Shiozawa, Ms. Tomoyo Kakita, and Ms. Kimie Nomura for their technical assistance, and Ms. Sayuri Sengoku for providing administrative assistance.

Author Contributions

Conceived and designed the experiments: KT HM. Performed the experiments: YT MS SS ES SH RA. Analyzed the data: YT MS HM KT. Contributed reagents/materials/analysis tools: RA TN. Wrote the paper: KT HM.

21. Bridge JA, Kanamori M, Ma Z, Pickering D, Hill DA, et al. (2001) Fusion of the ALK gene to the clathrin heavy chain gene, CLTC, in inflammatory myofibroblastic tumor. Am J Pathol 159: 411–415.
22. Ma Z, Hill DA, Collins MH, Morris SW, Sumegi J, et al. (2003) Fusion of ALK to the Ran-binding protein 2 (RANBP2) gene in inflammatory myofibroblastic tumor. Genes Chromosomes Cancer 37: 98–105.
23. Debiec-Rychter M, Marynen P, Hagemeijer A, Pauwels P (2003) ALK-ATIC fusion in urinary bladder inflammatory myofibroblastic tumor. Genes Chromosomes Cancer 38: 187–190.
24. Panagopoulos I, Nilsson T, Domanski HA, Isaksson M, Lindblom P, et al. (2006) Fusion of the SEC31L1 and ALK genes in an inflammatory myofibroblastic tumor. Int J Cancer 118: 1181–1186.
25. Delsol G, Lamant L, Mariame B, Pulford K, Dastugue N, et al. (1997) A new subtype of large B-cell lymphoma expressing the ALK kinase and lacking the 2; 5 translocation. Blood 89: 1483–1490.
26. Gascoyne RD, Lamant L, Martin-Subero JI, Lestou VS, Harris NL, et al. (2003) ALK-positive diffuse large B-cell lymphoma is associated with Clathrin-ALK rearrangements: report of 6 cases. Blood 102: 2568–2573.
27. Van Roosbroeck K, Cools J, Dierickx D, Thomas J, Vandenberghe P, et al. (2010) ALK-positive large B-cell lymphomas with cryptic SEC31A-ALK and NPM1-ALK fusions. Haematologica 95: 509–513.
28. Takeuchi K, Soda M, Togashi Y, Ota Y, Sekiguchi Y, et al. (2010) Identification of a novel fusion, SQSTM1-ALK, in ALK-positive large B-cell lymphoma. Haematologica.
29. Debelenko LV, Raimondi SC, Daw N, Shivakumar BR, Huang D, et al. (2011) Renal cell carcinoma with novel VCL-ALK fusion: new representative of ALK-associated tumor spectrum. Mod Pathol 24: 430–442.
30. Sugawara E, Togashi Y, Kuroda N, Sakata S, Hatano S, et al. (in press) Identification of ALK Fusions in Renal Cancer: Large-Scale Immunohistochemical Screening by intercalated Antibody-Enhanced Polymer Method. Cancer.
31. Du XL, Hu H, Lin DC, Xia SH, Shen XM, et al. (2007) Proteomic profiling of proteins dysregulted in Chinese esophageal squamous cell carcinoma. J Mol Med 85: 863–875.
32. Jazii FR, Najafi Z, Malekzadeh R, Conrads TP, Ziaee AA, et al. (2006) Identification of squamous cell carcinoma associated proteins by proteomics and loss of beta tropomyosin expression in esophageal cancer. World J Gastroenterol 12: 7104–7112.
33. Lin E, Li L, Guan Y, Soriano R, Rivers CS, et al. (2009) Exon array profiling detects EML4-ALK fusion in breast, colorectal, and non-small cell lung cancers. Mol Cancer Res 7: 1466–1476.
34. Martelli MP, Sozzi G, Hernandez L, Pettirossi V, Navarro A, et al. (2009) EML4-ALK rearrangement in non-small cell lung cancer and non-tumor lung tissues. Am J Pathol 174: 661–670.
35. Takeuchi K, Soda M, Togashi Y, Sugawara E, Hatano S, et al. (2011) Pulmonary inflammatory myofibroblastic tumor expressing a novel fusion, PPFIBP1-ALK: reappraisal of anti-ALK immunohistochemistry as a tool for novel ALK fusion identification. Clin Cancer Res 17: 3341–3348.
36. Travis WD, Brambilla E, Noguchi M, Nicholson AG, Geisinger KR, et al. (2011) International association for the study of lung cancer/american thoracic society/european respiratory society international multidisciplinary classification of lung adenocarcinoma. J Thorac Oncol 6: 244–285.
37. Yamamoto M, Takeuchi K, Shimoji M, Maniwa T, Isaka M, et al. (in press) Small non-mucinous bronchioloalveolar carcinoma with ALK immunoreactivity: A novel ALK fusion gene? Cancer Sci.
38. Takeuchi K, Choi YL, Soda M, Inamura K, Togashi Y, et al. (2008) Multiplex reverse transcription-PCR screening for EML4-ALK fusion transcripts. Clin Cancer Res 14: 6618–6624.
39. Choi YL, Takeuchi K, Soda M, Inamura K, Togashi Y, et al. (2008) Identification of novel isoforms of the EML4-ALK transforming gene in non-small cell lung cancer. Cancer Res 68: 4971–4976.
40. Onishi M, Kinoshita S, Morikawa Y, Shibuya A, Phillips J, et al. (1996) Applications of retrovirus-mediated expression cloning. Exp Hematol 24: 324–329.
41. Stenoien DL, Brady ST (1997) Immunochemical analysis of kinesin light chain function. Mol Biol Cell 8: 675–689.

42. Rahman A, Kamal A, Roberts EA, Goldstein LS (1999) Defective kinesin heavy chain behavior in mouse kinesin light chain mutants. J Cell Biol 146: 1277–1288.
43. Houtman SH, Rutteman M, De Zeeuw CI, French PJ (2007) Echinoderm microtubule-associated protein like protein 4, a member of the echinoderm microtubule-associated protein family, stabilizes microtubules. Neuroscience 144: 1373–1382.
44. Sablin EP (2000) Kinesins and microtubules: their structures and motor mechanisms. Curr Opin Cell Biol 12: 35–41.

BJUI
BJU INTERNATIONAL

Characteristics and clinical significance of prostate cancers missed by initial transrectal 12-core biopsy

Noboru Numao, Satoru Kawakami, Mizuaki Sakura, Soichiro Yoshida, Fumitaka Koga, Kazutaka Saito, Hitoshi Masuda, Yasuhisa Fujii, Shinya Yamamoto*, Junji Yonese*, Yuichi Ishikawa†, Iwao Fukui* and Kazunori Kihara

*Department of Urology, Graduate School, Tokyo Medical and Dental University, and Departments of *Urology and †Pathology, Cancer Institute Hospital, Japanese Foundation for Cancer Research, Tokyo, Japan*

Accepted for publication 21 April 2011

Study Type – Diagnostic (exploratory cohort)
Level of Evidence 3a

What's known on the subject? and What does the study add?
Initial transrectal 12-core biopsy has a small but definite risk of missing anterior significant prostate cancers irrespective of age, PSA, prostate volume and DRE findings.

Our study yields valuable information for diagnosis and treatment decision of prostate cancer based on transrectal 12-core biopsy.

OBJECTIVE

- To characterize prostate cancers missed by initial transrectal 12-core biopsy.

PATIENTS AND METHODS

- Between 2002 and 2008, 715 men with prostate-specific antigen levels in the range 2.5–20 ng/mL or abnormal digital rectal examination underwent three-dimensional 26-core prostate biopsy (i.e. a combination of transrectal 12-core biopsy and transperineal 14-core biopsy) on initial examination.
- Of the 257 patients diagnosed with cancer, 120 patients subsequently underwent radical prostatectomy.
- Cancers were grouped into TR12-negative cancers (i.e. not detected through transrectal 12-core biopsy but detected through transperineal 14-core biopsy) and TR12-positive (i.e. detected through transrectal 12-core biopsy) cancers.
- Clinicopathological characteristics of the TR12-negative and TR12-positive cancers were evaluated.

RESULTS

- TR12-negative cancers comprised 21% of the three-dimensional 26-core biopsy-detected cancers.
- The frequency of cancers with a biopsy Gleason score ≤6 and that of cancers with a biopsy primary Gleason grade ≤3 was higher in TR12-negative cancers, at 58% and 83%, respectively, than in TR12-positive cancers, at 25% ($P < 0.001$) and 53% ($P < 0.001$), respectively.
- The median number of positive cores in TR12-negative cancers was two out of 26.
- TR12-negative cancers were more frequently located anteriorly than posteriorly.
- The incidence of the TR12-negative cancers was not associated significantly with any clinical variable.

CONCLUSION

- Many of the cancers missed by initial transrectal 12-core biopsy are probably low-grade and low-volume diseases, although initial transrectal 12-core biopsy has a small but definite risk of missing anterior significant cancers.

KEYWORDS

biopsy, prostatectomy, prostatic neoplasm

INTRODUCTION

In a pattern consistent with the worldwide trend toward choosing extended over non-extended prostate biopsy methods, transrectal 12-core prostate biopsy (TR12PBx) is currently one of the most preferred biopsy methods for detecting prostate cancers. A systematic review of prostate biopsy methods noted that TR12PBx strikes a satisfactory balance with sufficiently high rates of cancer detection and sufficiently low rates of biopsy-associated comorbidity, and that taking more than 12 cores adds no significant benefit [1]. TR12PBx also meets the criteria for initial biopsy provided by the representative clinical guidelines [2,3]. Yet several studies have reported that repeat biopsy after negative initial extended transrectal biopsy detects prostate cancer in 17–21% of men [4–6], suggesting that these initial extended transrectal biopsies may miss a substantial number of cancers.

To clarify the incidence and clinical importance of cancers missed by TR12PBx, it is necessary to analyze the results obtained using biopsy protocols that include not only all of the TR12PBx sampling sites, but also

 | doi:10.1111/j.1464-410X.2011.10427.x

additional sampling sites. To the best of our knowledge, there are currently three biopsy protocols that meet these requirements. The first is three-dimensional 26-core prostate biopsy (3D26PBx), a combination of transperineal 14-core prostate biopsy (TP14PBx) and TR12PBx (Fig. 1), introduced by our group [7–9]. In a previous analysis of 321 men examined through 3D26PBx, we reported that 3D26PBx increased cancer detection by 24% compared to TR12PBx [7]. The second is transrectal 21-core biopsy [10]. The transrectal 21-core biopsy can detect significantly more cancers (increased detection of 9.8%) than the TR12PBx. The third is transrectal 14-core biopsy (TR12PBx plus two extreme anterior apical biopsy sites) [11]. The addition of only two extreme anterior apical sampling sites to TR12PBx increased the cancer detection rate by 7.5%. Although these studies mainly focused on cancer detectability, characteristics of cancers missed by TR12PBx have not been fully assessed to date.

When a patient undergoes an initial TR12PBx and the result is negative for cancer, how much risk does he have for a clinically important cancer that is missed? What are characteristics of the cancers missed by TR12PBx? To address these questions, we evaluated the characteristics of cancers that were detected or missed by TR12PBx in a cohort of 715 men undergoing 3D26PBx.

PATIENTS AND METHODS

PATIENTS

Between June 2002 and June 2008, 757 men prospectively underwent 3D26PBx as an initial biopsy at our institutions because of higher PSA levels >2.5 ng/mL and/or abnormal DRE findings in a clinical setting. Patients were excluded if they had diabetes mellitus or any rectal disease (e.g. uncontrolled hemorrhoids) because of the high risk of infection or rectal bleeding. In principle, those with apparently palpable mass, age ≥75 years, PSA level ≥20 ng/mL or poor state of health were excluded from recommendation for 3D26PBx. Written informed consent was obtained from all patients and 3D26PBx was performed under spinal, general or, recently, local anaesthesia [12], as described previously [7–9]. Of these 757 patients, 42 were excluded from the current study because of palpable stage T3/4 tumours, PSA level ≥20 ng/mL or lack of baseline clinical data. A total of 715 patients were subjected for analyses.

FIG. 1. Transverse, sagittal and coronal projections of three-dimensional 26-core prostate biopsy (3D26PBx), a combination of transperineal 14-core prostate biopsy (TP14PBx) and transrectal 12-core prostate biopsy (TR12PBx). The sampling sites are named: anterior 1 (A1), anterior 2 (A2), posterior 1 (P1), posterior 2 (P2), anterolateral (AL), posterolateral (PL) and transition zone (TZ) in TP14PBx; parasagittal apex (pa), parasagittal midprostate (pm), parasagittal base (pb), lateral apex (la), lateral midprostate (lm) and lateral base (lb) in TR12PBx.

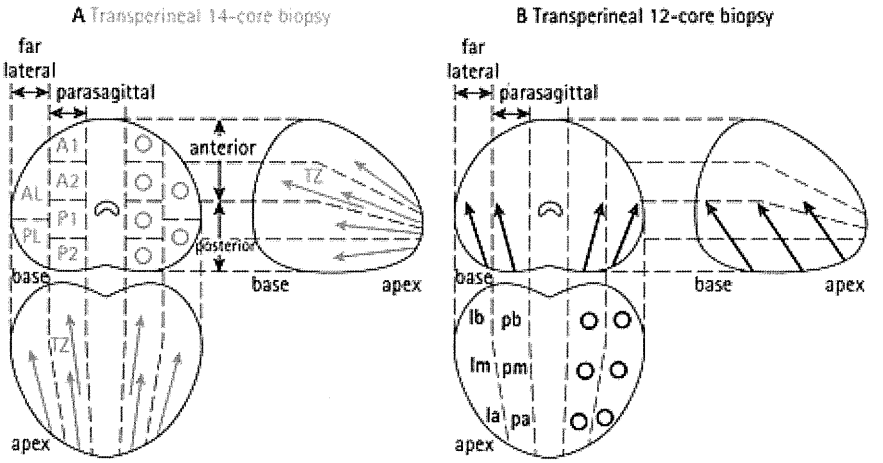

PATHOLOGICAL EVALUATION

All biopsy and radical prostatectomy (RP) specimens were re-evaluated by a single pathologist according to the 2005 International Society of Urologic Pathology Consensus Conference on Gleason Grading [3,13,14]. Each biopsy core was individually labelled so that the location of cancer-positive cores could be analyzed. All RP specimens were processed as described previously [9]. Tumour volume, Gleason score (GS), pathological stage and location of each isolated cancer focus in the RP specimens were recorded. Significant cancer was defined as a tumour volume ≥0.5 mL and/or Gleason pattern 4/5 and/or extraprostatic extension. A significant cancer focus was defined as one fulfilling the above-mentioned criteria for significant cancer, and was extensively evaluated. For analysis of cancer location, the prostate was divided into anterior, posterior and apical regions. The apical region was defined as the most inferior 10 mm of the gland. The remaining part of the gland was divided into anterior and posterior regions at the height of the urethra [15]. When a significant focus lay astride two regions, it was assigned to both regions.

DATA ANALYSIS

All cancers were grouped into two mutually exclusive groups: TR12-negative (i.e. not detected through transrectal 12-core biopsy but detected through transperineal 14-core biopsy) and TR12-positive (i.e. detected through transrectal 12-core biopsy) cancers. The former group did not have cancer-positive cores within the TR12PBx scheme but had cancer-positive cores within the TP14PBx scheme, and the latter had cancer-positive cores within the TR12PBx scheme. These two groups were compared with regard to patient age, PSA level, prostate volume, DRE findings, biopsy GS and the number of positive cores. In patients treated with RP, the two groups were also compared with regard to RP GS, pathological stage, tumour volume, frequency of significant cancer and cancer location. The study cohort was categorized by age, PSA level, prostate volume and DRE findings to identify any patient subgroups in which TR12PBx did not exhibit sufficient cancer detection rates.

STATISTICAL ANALYSIS

All analyses were performed using JMP, version 7 (SAS Institute Inc., Cary, NC, USA). Continuous variables were analyzed using Mann–Whitney's *U*-test. Categorical variables were analyzed using the chi-squared test or Fisher's exact test. The

TABLE 1 Patient and tumour characteristics

Variable	All patients ($n = 715$)	Patients with cancer ($n = 257$)	TR12-positve cancer ($n = 204$)	TR12-negative cancer ($n = 53$)	P
Age (years)	66 (61–71)	66 (63–72)	68 (63–72)	67 (63–73)	0.914
PSA level (ng/mL)	6.1 (4.7–8.5)	7.0 (5.1–9.6)	7.2 (5.1–9.8)	6.8 (5.2–8.7)	0.370
Prostate volume (mL)	35 (27–47)	29 (23–39)	29 (22–37)	32 (27–48)	0.003
% Abnormal DRE	16	25	29	11	0.009
Number of positive cores, *n* (range)	–	5 (2–8)	6 (3–9)	2 (1–2)	<0.001
Biopsy GS, *n* (%)					
5–6	–	83 (32)	52 (25)	31 (58)	<0.001
3 + 4	–	69 (27)	56 (27)	13 (25)	
4 + 3	–	44 (17)	39 (19)	5 (9)	
8 – 10	–	61 (24)	57 (28)	4 (8)	

Continuous variables are expressed as the median (interquartile range). GS, Gleason score; TR12-positive, transrectal 12-core biopsy-positive; TR12-negative, transrectal 12-core biopsy-negative

Transperineal sampling site*	% Cancer detection	P
A1	47	
A2	28	
AL	28	
P1	24	
P2	19	
PL	19	
TZ	19	
A1 + A2	62	0.0201†
P1 + P2	40	
A1 + A2 + AL	75	0.0091†
P1 + P2 + PL	51	

TABLE 2 TR12-negative cancer (n = 53) detection rates in each transperineal sampling site

**See Fig. 1. †According to a chi-squared test (A1 + A2 vs P1 + P2, A1 + A2 + AL vs P1 + P2 + PL). TR12-negative, transrectal 12-core biopsy-negative.*

Cochran–Armitage test was used to test for trends. $P < 0.05$ was considered statistically significant.

RESULTS

CHARACTERISTICS OF TR12-NEGATIVE CANCERS: ANALYSES ON BIOPSY SPECIMENS

Prostate cancers were detected through 3D26PBx in 257 (35.9%) of the 715 men. Of these 257 cancers, 53 (21%) were identified as TR12-negative cancers; in other words, the addition of the TP14PBx sites to the TR12PBx sites improved the cancer detection rate by 26%. Patient and tumour characteristics of TR12-positive and TR12-negative cancers are shown in Table 1. Compared to patients with TR12-positive cancers, patients with TR12-negative cancers had significantly larger prostates and a lower incidence of abnormal DRE. The frequency of cancers with biopsy GS ≤6 and that of cancers with biopsy primary Gleason grade ≤3 were higher in TR12-negative cancers, at 58% and 83%, respectively, than in TR12-positive cancers, at 25% ($P < 0.001$) and 53% ($P < 0.001$), respectively.

In the 53 TR12-negative cancers, cancer-positive rates within the TP14PBx sampling sites are shown in Table 2. The farthest anterior sampling site (A1; Fig. 1) had the highest cancer-positive rate of 47%. There were six cores from the anterior sampling sites (A1, A2 and AL; Fig. 1) that detected significantly ($P = 0.009$) more cancers than six cores from the posterior sites (P1, P2 and PL; Fig. 1), indicating that TR12-negative cancers are located more frequently in the anterior region than in the posterior region.

CHARACTERISTICS OF TR12-NEGATIVE CANCERS: ANALYSES ON RP SPECIMENS

In total, 120 of the 257 (47%) patients underwent RP [16]. Characteristics of TR12-positive and TR12-negative cancers are shown in Table 3. Among the pathological variables analyzed in the RP cohort, the TR12-positive and TR12-negative groups differed with respect to cancer location: specifically, TR12-negative cancers were located less frequently in the posterior region than the TR12-positive cancers.

SUBGROUPS IN WHICH TR12PBX IS INSUFFICIENT FOR CANCER DETECTION

To identify patient subgroups in which TR12PBx would be entirely insufficient for cancer detection and in which more sampling would be needed, we compared the incidence of TR12-negative cancers in subgroups defined by age, PSA level, prostate volume or DRE findings (Fig. 2). Although cancer detection rates of 3D26PBx were significantly higher in patient subgroups with higher age, higher PSA level, smaller prostates or abnormal DRE findings, the incidence of TR12-negative cancers did not differ significantly between any of the subgroups.

COMPARISON OF CANCER CHARACTERISTICS BETWEEN NORMAL AND ABNORMAL DRE GROUPS

PSA screening has significantly increased the proportion of men who undergo prostate biopsy based on PSA findings alone. To evaluate the efficacy of TR12PBx in men with normal DRE in more detail, the cancer characteristics of TR12-negative cancers were analyzed according to DRE findings (Table 4). TR12-positive cancers in the normal DRE group tended to have lower biopsy cancer grade and fewer positive cores compared to those in the abnormal DRE group. By contrast, in TR12-negative cancers, biopsy cancer grade and the number of positive cores did not differ significantly between the groups.

DISCUSSION

In the present study, we evaluated the characteristics of cancers missed by initial TR12PBx, more precisely, cancers missed by TR12PBx in patients who underwent 3D26PBx (TR12-negative cancers), and thus

showed the diagnostic performance of TR12PBx. Initial TR12PBx missed 21% of cancers that were detectable through 3D26PBx; however, it should be noted that more than half of TR12-negative cancers had a biopsy GS ≤6, and most of them had a biopsy primary Gleason grade ≤3. Furthermore, the median number of positive cores in TR12-negative cancers was only two out of 26, suggesting that a substantial number of TR12-negative cancers can be expected to be low-grade and low-volume diseases.

Although our RP cohort is highly selective, most TR12-negative cancers treated with RP were significant cancers. Yet 87% were organ-confined disease and 75% were primary Gleason grade 3 cancers with favourable prognosis. Combined with the biopsy findings, this indicates that TR12-negative cancers have lower malignant potential than TR12-positive cancers, and that most of them can be expected to be organ confined, although a small number of TR12-negative cancers appear to be significant cancers that would exhibit biological aggressiveness.

The characteristics of the location of TR12-negative cancers are clearly shown in the present study. Our analysis of positive transperineal sites in TR12-negative cancers confirmed that TR12-negative cancers were located in the anterior portion of the gland rather than the posterior portion. The cancer location of TR12-negative cancers in RP specimens also supports this notion, suggesting that TR12PBx would be insufficient to detect anterior cancers. The results obtained in the present study are similar to those obtained by Moussa *et al.* [11], who reported that the addition of only two extreme anterior apical cores to TR12PBx transrectal sampling improved cancer detection by 7.5% and that these two cores achieved the highest rate of unique cancer detection. They therefore introduced the 14-core biopsy scheme (TR12PBx biopsy plus two extreme apical cores) as an initial biopsy to detect more anterior apical cancers.

On the basis of these findings, simply adding more transrectal sampling sites from the bottom of the prostate gland to TR12PBx would not increase its cancer detection rate efficiently. Indeed, several studies have tested transrectal extended biopsy methods using more than 12 cores; however, most of these so-called 'saturation' transrectal biopsy protocols did not outperform TR12PBx [17–19]. The transrectal 21-core biopsy [10] can identify more cancers than TR12PBx can, although the 9.8% increase in cancer detection that results from the nine additional samplings appears to be inefficient. In the present study, the addition of two far-anterior transperineal sampling to the TR12PBx improved its cancer detection rate by 11%. From these results, we consider that a few additional samplings in the anterior apical portion are effective for detecting cancers missed by TR12PBx.

In recent analyses on men with a PSA level <20 ng/mL without locally advanced tumours on DRE findings, there were no significant differences among subgroups defined by age, PSA level, prostate volume or DRE in the incidence of TR12-negative cancers. Therefore, we could not identify any subgroup in which TR12PBx would be entirely insufficient for cancer detection and in which more sampling would therefore be needed. There is the potential concern that TR12PBx may probably miss anterior aggressive cancers in men with normal DRE, although our analysis of cancer characteristics according to DRE findings shows that a large proportion of TR12-negative cancers probably consist of low-grade and low-volume disease, regardless of DRE findings. We consider that these results are sufficient grounds to eliminate such concerns.

Recently, the value of MRI for detecting prostate cancers and determining their location has been extensively studied [20]. Lawrentschuk *et al.* [21] retrospectively analyzed patients with anteriorly predominant tumours on MRI who had undergone prostate biopsy and reported that MRI would be useful in the detection of

TABLE 3 Patient and tumour characteristics of 120 men undergoing radical prostectomy

Variable	TR12-positive cancer (*n* = 104/204)	TR12-negative cancer (*n* = 16/53)	*P*
Clinical			
Age (years)	67 (62–71)	64 (60–70)	0.245
PSA level (ng/mL)	6.7 (5.2–9.3)	6.4 (4.7–8.4)	0.362
Prostate volume (mL)	28 (22–34)	29 (20–38)	0.817
% Abnormal DRE	24	25	0.666
Biopsy			
Number of positive cores, *n* (range)	5 (3–9)	2 (1–3)	<0.001
GS, *n* (%)			
5–6	17 (16)	8 (50)	<0.001
3 + 4	32 (31)	5 (31)	
4 + 3	27 (26)	1 (6)	
8–10	28 (27)	2 (13)	
Radical protectomy			
GS, *n* (%)			
5–6	26 (25)	3 (19)	<0.001
3 + 4	49 (47)	9 (56)	
4 + 3	16 (15)	3 (19)	
8–10	13 (13)	1 (6)	
% Organ-confined disease	73	87	0.178
% Tumour volume ≥0.5 mL	80	75	0.437
% Significant cancer	92	87	0.396
Significant cancer			
% Located posteriorly	83	50	<0.001
% Located anteriorly	75	71	0.500
% Located apically	86	79	0.331

Continuous variables are expressed as the median (interquartile range). GS, Gleason score; TR12-positive, transrectal 12-core biopsy-positive; TR12-negative, transrectal 12-core biopsy-negative.

anterior tumours that are difficult to detect using transrectal biopsy. It appears that MRI is a promising tool for detecting anterior cancers, although its cost is high.

Pathological evaluation in the present study is based on the 2005 International Society of Urologic Pathology Consensus [13,14]. Fused glands, ill-defined glands with poorly formed glandular lumina and most of the cribriforms are previously categorized into Gleason pattern 3 but, in the 2005 consensus, are categorized into Gleason pattern 4. Furthermore, two new modifications to the Gleason scoring system are recommended in the evaluation of biopsy specimens. One is that any high-grade pattern, no matter how small quantitatively, should be incorporated into the GS, although any secondary grade that occupies <5% of the specimen would not have been reported under the previous system. The other modification is that all higher tertiary grade components of the tumour, which were previously ignored, should be incorporated into the GS. Accordingly, the rates of high-grade patterns scored according to the 2005 consensus are higher than those scored under the previous system. This phenomenon has been confirmed in a study by Billis *et al.* [22] showing that GS that had been scored under the previous system were upgraded by re-evaluation under the 2005 consensus in 26.7% of the biopsy specimens. Similarly, the GS of some of the patients in the present study would have been lower if they had been evaluated under the previous system. We consider that these findings strengthen our view that many TR12-negative cancers can be expected to be low-grade diseases.

FIG. 2. Bar graphs show detection rates of cancers of all types through 3D26PBx. The overlying line plots show detection rates of TR12-negative cancers (i.e. not detected through transrectal 12-core biopsy but detected through transperineal 14-core biopsy). Statistical analyses were performed using the Cochran–Armitage trend test.

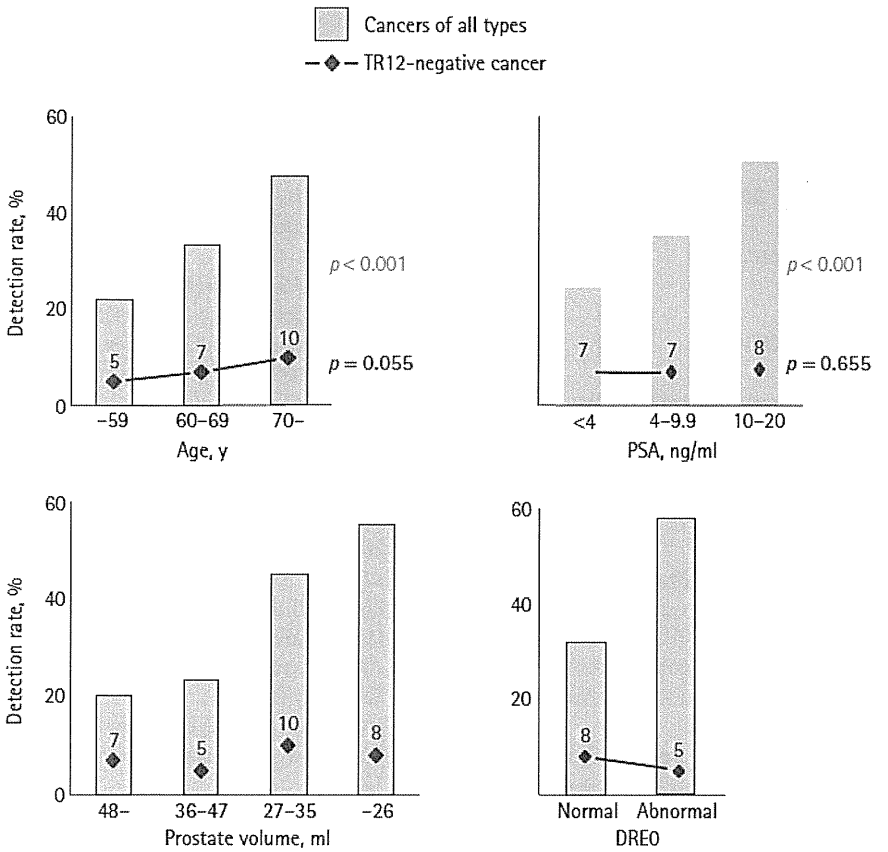

The present study does not indicate that we should aim to actively detect TR12-negative cancers in all candidates for initial prostate biopsy because a substantial number of TR12-negative cancers are low-grade and low-volume diseases. Overdiagnosis and

overtreatment are now issues of major concern in the management of prostate cancer. Draisma *et al.* [23] have reported that the rate of overdiagnosis of prostate cancer has been estimated at 23–66% of screening-detected cancers. The main purpose of prostate biopsy is not only to detect more prostate cancers, but also to detect more life-threatening cancers. Even if we missed a case of prostate cancer at an initial biopsy, we would be able to determine the need for a repeat biopsy through the PSA test in most cases, and most cancers detected by repeat biopsy are manageable and not life-threatening [24]. If the goal of screening were simply to detect life-threatening cancers, the addition of sampling sites to the TR12PBx protocol would not be essential in all candidates for initial biopsy.

Another important purpose of biopsy, however, is to accurately characterize any tumours to allow for a more informed treatment decision-making process. If a custom treatment is to be devised for each individual patient, more sampling is required to generate more information, although more sampling leads to a greater detection of indolent cancers. This clinical dilemma makes it difficult to determine the optimal biopsy scheme. We now consider that the addition of anterior sampling sites to the initial TR12PBx would be a reasonable option for younger men with a long life expectancy or for men with suspected anterior cancer as assessed by MRI. On the basis of the analysis in subgroups divided by DRE findings, the finding that a DRE was normal does not mean that additional sampling of the anterior prostate should be performed. At repeat biopsy after negative TR12PBx, however, anterior samplings are highly recommended.

The present study has several limitations that should be considered. Given that 3D26PBx does not identify all cancers, it is possible that TP12PBx may fail to detect an even greater percentage of cancers than reported in the present study. We recommend transperineal sampling for the detection of TR12-negative cancers, although we realize that the transperineal approach may be unfamiliar to many urologists. A recently reported technique for simple and effective local anaesthesia would render transperineal extended biopsy more feasible [12]. Furthermore, because of the limited duration of the follow-up in the present study, we could not report the oncological outcome of TR12-negative cancers. Long-term observation will be required to acquire a better understanding of the diagnostic performance of TR12PBx.

In conclusion, TR12PBx missed 21% of cancers that were detected by 3D26PBx on initial biopsy. Although many of the undetected cancers were expected to be low-grade and low-volume diseases, it should be noted that the initial TR12PBx has a small but definite risk of missing anterior significant cancers.

CONFLICT OF INTEREST

None declared.

REFERENCES

1 **Eichler K, Hempel S, Wilby J, Myers L, Bachmann LM, Kleijnen J.** Diagnostic value of systematic biopsy methods in the investigation of prostate cancer: a systematic review. *J Urol* 2006; **175**: 1605–12

2 **NCCN Clinical Practice Guideline in Oncology.** Prostate Cancer Early Detection. V.2.2010. Available at: http://www.nccn.org/professionals/physician_gls/f_guidelines.asp. Accessed October 2010

3 **Heidenreich A, Bolla M, Joniau S *et al.*** Guidelines on Prostate Cancer 2010. Available at: http://www.uroweb.org/gls/pdf/08_Prostate_Cancer.pdf. Accessed October 2010

4 **Campos-Fernandes JL, Bastien L, Nicolaiew N *et al.*** Prostate cancer detection rate in patients with repeated extended 21-sample needle biopsy. *Eur Urol* 2009; **55**: 600–6

5 **Philip J, Hanchanale V, Foster CS, Javlé P.** Importance of peripheral biopsies in maximising the detection of early prostate cancer in repeat 12-core biopsy protocols. *BJU Int* 2006; **98**: 559–62

6 **Singh H, Canto EI, Shariat SF *et al.*** Predictors of prostate cancer after initial negative systematic 12 core biopsy. *J Urol* 2004; **171**: 1850–4

7 **Kawakami S, Hyochi N, Yonese J *et al.*** Three-dimensional combination of transrectal and transperineal biopsies for efficient detection of stage T1c prostate cancer. *Int J Clin Oncol* 2006; **11**: 127–32

8 **Kawakami S, Okuno T, Yonese J *et al.*** Optimal sampling sites for repeat prostate biopsy: a recursive partitioning analysis of three-dimensional 26-core systematic biopsy. *Eur Urol* 2007; **51**: 675–82

9 **Numao N, Kawakami S, Yokoyama M *et al.*** Improved accuracy in predicting the presence of Gleason pattern 4/5 prostate cancer by three-dimensional 26-core systematic biopsy. *Eur Urol* 2007; **52**: 1663–8

10 **Guichard G, Larré S, Gallina A *et al.*** Extended 21-sample needle biopsy protocol for diagnosis of prostate cancer in 1000 consecutive patients. *Eur Urol* 2007; **52**: 430–5

11 **Moussa AS, Meshref A, Schoenfield L *et al.*** Importance of additional 'extreme' anterior apical needle biopsies in the initial detection of prostate cancer. *Urology* 2010; **75**: 1034–9

12 **Kubo Y, Kawakami S, Numao N *et al.*** Simple and effective local anesthesia for transperineal extended prostate biopsy: application to three-dimensional 26-core biopsy. *Int J Urol* 2009; **16**: 420–3

13 **Epstein JI, Allsbrook WC Jr, Amin MB, LL E, Grading ISUP.** Committee. The 2005 International Society of Urological Pathology (ISUP) Consensus Conference on Gleason Grading of Prostatic Carcinoma. *Am J Surg Pathol* 2005; **29**: 1228–42

14 **Srigley JR, Amin MB, Epstein JI *et al.*** Updated protocol for the examination of specimens from patients with carcinomas of the prostate gland. *Arch Pathol Lab Med* 2006; **130**: 936–46

15 **Koppie TM, Bianco FJ Jr, Kuroiwa K *et al.*** The clinical features of anterior prostate cancers. *BJU Int* 2006; **98**: 1167–71

16 **Kawakami S, Fukui I, Yonese J *et al.*** Antegrade radical retropubic prostatectomy with preliminary ligation of vascular pedicles in 614 consecutive patients. *Jpn J Clin Oncol* 2007; **37**: 528–33

17 **Jones JS, Patel A, Schoenfield L, Rabets JC, Zippe CD, Magi-Galluzzi C.** Saturation technique does not improve cancer detection as an initial prostate biopsy strategy. *J Urol* 2006; **175**: 485–8

18 **Pepe P, Aragona F.** Saturation prostate needle biopsy and prostate cancer detection at initial and repeat evaluation. *Urology* 2007; **70**: 1131–5
19 **Scattoni V, Roscigno M, Raber M *et al.*** Initial extended transrectal prostate biopsy – are more prostate cancers detected with 18 cores than with 12 cores? *J Urol* 2008; **179**: 1327–31
20 **Villers A, Puech P, Mouton D, Leroy X, Ballereau C, Lemaitre L.** Dynamic contrast enhanced, pelvic phased array magnetic resonance imaging of localized prostate cancer for predicting tumor volume: correlation with radical prostatectomy findings. *J Urol* 2006; **176**: 2432–7
21 **Lawrentschuk N, Haider MA, Daljeet N *et al.*** 'Prostatic evasive anterior tumours': the role of magnetic resonance imaging. *BJU Int* 2010; **105**: 1231–6
22 **Billis A, Guimaraes MS, Freitas LL, Meirelles L, Magna LA, Ferreira U.** The impact of the 2005 international society of urological pathology consensus conference on standard Gleason grading of prostatic carcinoma in needle biopsies. *J Urol* 2008; **180**: 548–52
23 **Draisma G, Etzioni R, Tsodikov A *et al.*** Lead time and overdiagnosis in prostate-specific antigen screening: importance of methods and context. *J Natl Cancer Inst* 2009; **101**: 374–83
24 **Schröder FH, van den Bergh RC, Wolters T *et al.*** Eleven-year outcome of patients with prostate cancers diagnosed during screening after initial negative sextant biopsies. *Eur Urol* 2010; **57**: 256–66

Correspondence: Noboru Numao, Department of Urology, Tokyo Medical and Dental University Graduate School, 1-5-45 Yushima, Bunkyo-ku, Tokyo 113-8519, Japan.
e-mail: noboru.uro@tmd.ac.jp

Abbreviations: **3D26PBx**, three-dimensional 26-core prostate biopsy; **GS**, Gleason score; **RP**, radical prostatectomy; **TR12PBx**, transrectal 12-core prostate biopsy; **TP14PBx**, transperineal 14-core prostate biopsy.